To the Graduate Council:

I am submitting herewith a thesis written by Yeunsik Choi entitled "Thermal Radiation Effects in Laminar Natural Convection Plumes above Horizontal Line Heat Sources with and without an Adiabatic Vertical Wall." I have examined the final copy of this thesis for form and content and recommend that it be accepted in partial fulfillment of the requirements for the degree of Master of Science, with a major in Engineering Science.

Kenneth H. Kim, Major Professor

We have read this thesis
and recommend its acceptance:

John H Forester

Osama Soliman

Accepted for the Council:

Vice Provost
and Dean of The Graduate School

STATEMENT OF PERMISSION TO USE

In presenting this thesis in partial fulfillment of the requirements for a Master's degree at The University of Tennessee, Knoxville, I agree that the Library shall make it available to borrowers under rules of the Library. Brief quotations from this thesis are allowable without special permission, provided that accurate acknowledgment of source is made.

Permission for extensive quotation from or reproduction of this thesis may be granted by my major professor, or in his absence, by the Head of Interlibrary Services when, in the opinion of either, the proposed use of the material is for scholarly purposes. Any copying or use of the material in this thesis for financial gain shall not be allowed without my written permission.

Signature Younsik Choi

Date May 28, 1985

THERMAL RADIATION EFFECTS IN LAMINAR NATURAL CONVECTION PLUMES ABOVE HORIZONTAL LINE HEAT SOURCES WITH AND WITHOUT AN ADIABATIC VERTICAL WALL

A Thesis

Presented for the

Master of Science

Degree

The University of Tennessee, Knoxville

Yeunsik Choi

June 1985

ACKNOWLEDGMENTS

The author wishes to express appreciation to his committee chairperson and major professor, Dr. Kenneth, H. Kim, professor of Engineering Science and Mechanics, for his academic and emotional support throughout this study and the entire graduate program.

Special gratitudes are given to his committee members, Dr. J. H. Forrester, professor of Engineering Science and Mechanics, and Dr. M. O. Soliman, associate professor of Engineering Science and Mechanics, for their constructive criticism and suggestions.

The author wishes to express appreciation to the Department of Engineering Science and Mechanics for their continued support for his graduate studies. Special thanks is given to Soyeon Shim for her typing and proofreading.

The author would like to extend his deepest gratitude to his parents and brothers for their encouragement and support throughout the study.

ABSTRACT

The purpose of this study is to investigate a steady laminar natural convection plume arising from a horizontal line source of heat. This study also includes a natural convection flow over a vertical adiabatic surface with a heat source concentrated at the leading edge. In each case, particular interest is directed to the examiation of the effect of thermal radiation heat transfer. The study is initiated by first determining a set of governing equations for an incompressible, Newtonian fluid in a two dimensional flow field where the no slip condition on the wall is applied. Fluid properties such as viscosity and thermal conductivity are assumed to be constant. Transformation variables, derived by Birkoff's group theory, reduce the governing partial differential equations to ordinary differential equations. The radiation properties of the medium are specified by assuming the medium is optically thick, which is known as the Rosseland approximation. The radiation heat flux which results from the Rosseland approximation is linearized.

The technique of numerical analysis used is the Runge-Kutta algorithm with Gill coefficients. This algorithm is employed in a program designed to generate solutions based on automatic corrections to initial guesses for starting values given to the slopes of the velocity and temperature profiles. The corrections are obtained by satisfying the asymptotic boundary layer conditions so that the mean square error between the computed variables and the asymptotic values is minimized.

Extensive numerical calculations are carried out for Prandtl

numbers ranging from 0.01 to 100 in the presence of and in the absence of thermal radiation. The results obtained from this research are plotted and analyzed.

TABLE OF CONTENTS

CHAPTER PAGE

I. INTRODUCTION.....1

II. THEORETICAL DEVELOPMENT.....6

A. Boundary Layer Equations.....6

B. Boundary Conditions.....17

III. ANALYSIS OF THE SIMILARITY SOLUTION.....21

A. Satisfaction of the Asymptotic Boundary Conditions.....21

B. The Solution Algorithm.....29

C. Results.....36

IV. CONCLUSIONS AND RECOMMENDATIONS.....39

LIST OF REFERENCES.....42

APPENDIXES.....45

APPENDIX A. Additional Figures.....46

APPENDIX B. Additional Tables.....57

APPENDIX C. Fortran Program.....60

VITA.....68

LIST OF TABLES

TABLE PAGE

1. The Values of the Maximum Error, DX, and CPU Time for Case I.....31
2. The Values of the Maximum Error, DX, and CPU Time for Case II.....32
3. The Values of the Maximum Error, DX, and CPU Time for Case III.....33
4. The Values of the Maximum Error, DX, and CPU Time for Case IV.....34
5. Comparison of Numerical Values of Computed Dimensionless Velocity f'(0) for Case I.....57
6. The Dimensionless Shear Stress on the Vertical Wall.....58
7. Comparison of The Effect of an Adiabatic Vertical Wall on Temperature Gradients for the First and Third Cases.....59

LIST OF FIGURES

FIGURE PAGE

1. Coordinate Systems..... 7
2. Visualized Procedure of All Cases.....35
3. Computed Value of f for Case I.....46
4. Computed Velocity Profiles for Case I.....47
5. Computed Temperature Distribution for Case I.....47
6. Computed Value of f for a Range of Prandtl Numbers by Gebhart et al.....48
7. Computed Value of Velocity Profiles for a Range of Prandtl Numbers by Gebhart et al.....48
8. Computed Temperature Distribution for a Range of Prandtl Numbers by Gebhart et al.....48
9. Computed Velocity Profiles for Case II (Pr=10.0).....49
10. Computed Temperature Distribution for Case II (Pr=10.0).....49
11. Computed Velocity Profiles for Case II (Pr=1.0).....50
12. Computed Temperature Distribution for Case II (Pr=1.0).....50
13. Computed Velocity Profiles for Case II (Pr=0.1).....51
14. Computed Temperature Distribution for Case II (Pr=0.1).....51
15. Computed Velocity Profiles for Case III.....52
16. Computed Temperature Distribution for Case III.....52
17. Computed Velocity Profiles for Case IV (Pr=10.0).....53
18. Computed Temperature Distribution for case IV (Pr=10.0).....53
19. Computed Velocity Profiles for Case IV (Pr=1.0).....54
20. Computed Temperature Distribution for Case IV (Pr=1.0).....54

FIGURE PAGE

21. Computed Velocity Profiles for Case IV (Pr=0.1).....55

22. Computed Temperature Distribution for Case IV (Pr=0.1).....55

23. Temperature Gradients across the Boundary Layer for Case I.....56

24. Temperature Gradients across the Boundary Layer for Case III.....56

LIST OF SYMBOLS

a_λ	absorption coefficient
A	variable as defined by equation (2-23)
B	variable as defined by equation (2-32)
C_p	specific heat of the fluid at constant pressure
E_{max}	maximum error
f	nondimensional stream function
$Gr_x = \frac{g\beta x^3 (T_o - T_\infty)}{\nu^2}$	Grashof number
k	thermal conductivity of the fluid
k_λ	optical thickness or opacity
K	absorptivity
K_λ	extinction coefficient of the fluid
l_m	extinction mean free path
n	exponent defined by equation (2-23)
$N = \frac{kK}{4\lambda^2 \sigma T_\infty^3}$	conduction-to-radiation parameter
p	pressure
$Pr = \frac{\nu}{\alpha}$	Prandtl number
$q_r = -\frac{4\lambda^2 \sigma}{3K} \frac{\partial T^4}{\partial y}$	radiative heat flux
Q	heat generated by the line heat source
S	coordinate along path of radiation
S^*	dummy variable of integration
T	fluid temperature

T_o	fluid temperature at $\eta = 0$
T_∞	freestream temperature
u	velocity component in x direction
v	velocity component in y direction
x	vertical height above the line heat source
y	horizontal distance from the mid-plane of the plume
z	value of initial guess
$\alpha = \frac{k}{\rho C_p}$	thermal diffusivity
β	coefficient of volume expansion
$\phi = \frac{T - T_\infty}{T_o - T_\infty}$	nondimensional temperature
ρ	fluid density
λ	thermal radiation wave length
σ	Stefan-Boltzman constant
σ_λ	scattering coefficient
ξ	similarity variable defined by equation (2-20)
$\eta = \frac{y}{x}\sqrt[4]{\frac{Gr_x}{4}}$	similarity variable defined by equation (2-19) (measure of distance from the wall)
ψ	stream function
μ	dynamic viscosity of the fluid
$\nu = \frac{\mu}{\rho}$	kinematic viscosity of the fluid

Subscripts:

z	denotes partial differentiation with respect to z
edge	edge of boundary layer
λ	wavelength-dependent

Superscript:

$'$ denotes differentiation with respect to η.

CHAPTER I

INTRODUCTION

Two-dimensional laminar boundary layer flow and convective heat transfer have been studied by many investigators; not much attention has been given, however, to cases where thermal radiation becomes an additional factor. Recent developments in hypersonic flight, missile or space shuttle re-entry, rocket combustion chambers, power plants for interplanetary flight and gas-cooled nuclear reactors have focused attention on thermal radiation as a mode of energy transfer, and emphasized the need for an improved understanding of radiative transfer in these processes.

This study concerns the natural convection plumes arising from a horizontal line source of heat in quiescent surroundings of infinite extent. The research also includes the investigation of a natural convection flow over a vertical adiabatic surface with a heat source concentrated at the leading edge. Numerous papers related to this subject were published since 1930. Gebhart et al. discuss the historical background in their paper [1]. In 1963, Fujii [3] published a thorough study about the natural convection plume above a horizontal line point heat source to which later experimental papers referred for comparison. Fujii solved the two dimensional flow configuration, assuming boundary behavior, in closed form for a Prandtl number (Pr) of 2, and for the axisymmetric case for Pr=1 and 2. He also used numerical intergration to solve the differential equations for Prandtl numbers of

0.01,0.7 and 10.0. Two experimental investigations into the velocity and temperature profiles around a horizontal wire in air are those by Brodowicz and Kierkus [14] in 1966 and by Forstrom and Sparrow [11] in 1967. Their results are only in fair agreement with the plume theory.

Gebhart, Pera and Schorr [1] published a paper related to steady laminar natural convection plumes above a horizontal line heat source (1970). Their investigation, for the first time, states the problem in the simplest variables, resolves various apparent redundancies in boundary conditions and indicates the optimum way to formulate this boundary value problem. In 1970, Schorr and Gebhart performed an experimental investigation of natural convection wakes above a line heat source [2]. This study presents the results of a carefully controlled experiment which for the first time had been done in a liquid having Prandtl number around 6.7 (similar to water), using an inferometer to give an accurate record of the entire temperature field at any given instant. The experimental results show good agreement with the theoretical similarity solution obtained from the numerical solution of the governing equations.

Kim and Ozisik published several papers in this field, especially in the area of thermal radiation effects in boundary layer flow [7,8], and Diggs and Kim [13] presented curvature effects on heat transfer in the free jet boundary. In 1982, Galuska and Kim [12], studied laminar natural convection heat transfer for non-Newtonian fluids. Particularly, the investigation centered on the momentum and heat transfer with thermal radiation influence. The technique used to solve

the tranformed ordinary equations was based on the Runge-Kutta algorithm with Gill coefficients [6,15].

A boundary layer problem concerned with the effects of thermal radiation on the temperature distribution and the heat transfer in an absorbing and emitting media flowing over a wedge was studied by Viskanta and Grosh [14]. In this paper, the general boundary-layer problem is formulated in terms of an equation of transfer for thermal radiation, a nonlinear integro-differential equation which represents conservation of energy, and the usual equations for conservation of mass and momentum. Because no general solution for this equation is possible, the Rosseland approximation for the radiant heat flux vector is used to simplify the energy equation. Especially, the results are presented for a fluid whose Prandtle number is 1, as well as for molten Pyrex glass.

Above mentioned studies [7, 8, 9, 12, 13] have shown that thermal radiation affects heat transfer both directly and indirectly. Radiant energy can be directly absorbed or emitted by a surface, and thereby alter its heat transfer characteristics. Indirectly, thermal radiation can be partially absorbed in the boundary layer, altering the temperature distribution, and thereby influencing the conductive and convective heat transfer characteristics.

The present study will not only confirm the previous study done by Gebhart et al. for the case of no radiation effects but, also will extend to the case of a natural convection flow over a vertical adiabatic surface with a heat source concentrated at the leading edge.

Futhermore, this study demonstrates the thermal radiation effect on the temperature and velocity profiles.

The following four cases will be studied in this research:

CASE I : Steady laminar natural convection plumes above a horizontal line heat source without thermal radiation.

CASE II : Steady laminar natural convection plumes above a horizontal line heat source with thermal radiation.

CASE III: Steady laminar natural convection plumes without thermal radiation over a vertical adiabatic surface with a heat source concentrated at the leading edge.

CASE IV : Steady laminar natural convection plumes with thermal radiation over a vertical adiabatic surface with a heat source concentrated at the leading edge.

Since the complexity introduced by radiative contribution to the energy flux is in part due to the dependence of the flux on the geometrical configuration of the problem, the simple geometry of a vertical plate is chosen for the third and fourth cases.

In the present investigation, the development of the momentun and energy equations in the boundary layer are first discussed, along with the similarity transformations. Then the analysis of the similarity solution will be discussed in detail (in Chapter II). When energy transfer by radiation and convection is present, the law of conservation of energy becomes a complicated nonlinear integro-differential equation. Thus, an exact analysis of the interaction of a radiation field with

absorbing and emitting media in the laminar boundary layer is a very difficult problem. For this reason the Rosseland approximation, which is valid for an optically thick medium, is used in this research to approximate the radiant-energy flux term. The strongly absorbing medium is of interest as it provides a physically significant standard of comparison for understanding the general case, and the author is of the opinion that the simple problem must be solved first before the more difficult problem can be attempted. In order to completly specify the problem, proper boundary conditions for the transformed governing equations are established for each case.

The technique used for numerical computation is the modified Runge-Kutta algorithm with Gill coefficients. This algorithm is used to generate solutions based on the self-adjusting technique to the initial guesses of the velocities and the heat flux. This numerical computational method will be discussed in Chapter III.

The results include the graphs depicting similarity forms of the temperature and velocity distributions for various Prandtl numbers (Pr) and conduction-to-radiation parameters (N). Other useful results are presented in tabular form. Conclusions and recommendations are included in the last chapter and the computer codes used in this analysis are listed in the Appendix C.

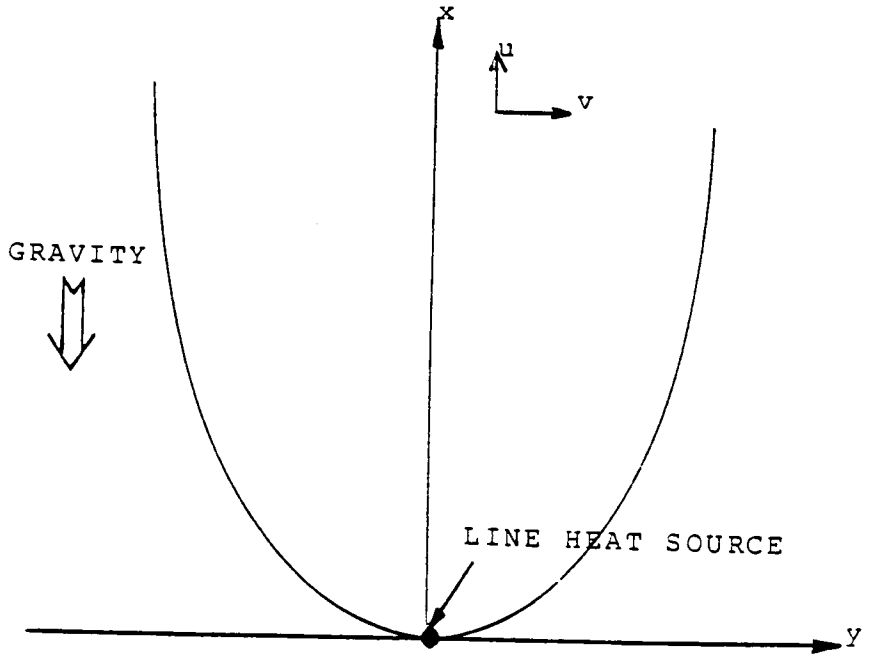
CHAPTER II

THEORETICAL DEVELOPMENT

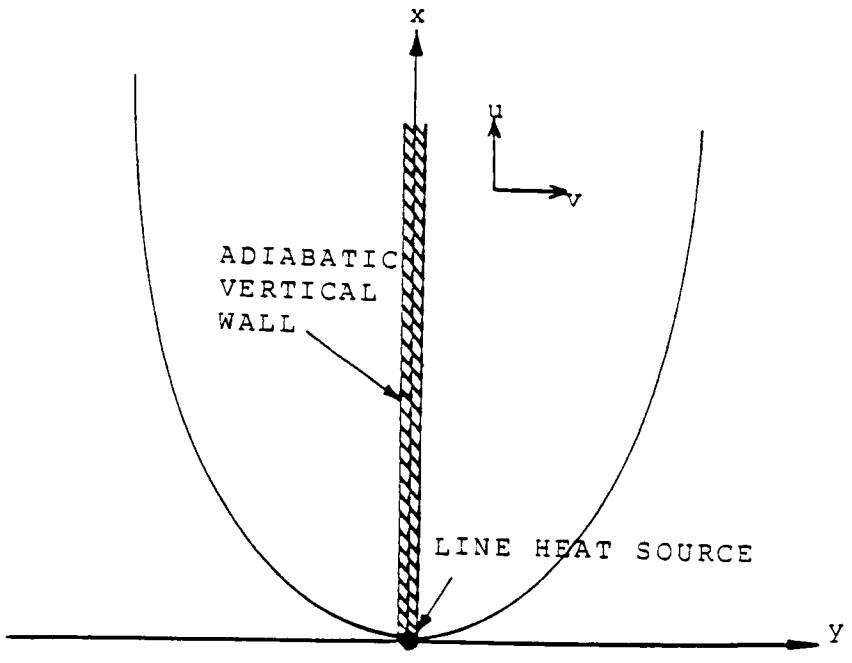
A. BOUNDARY LAYER EQUATIONS

The analysis of the convection region arising from a horizontal line source of heat can be divided into four regions: the limiting conduction region around the wire, the non-boundary layer region, the two-dimensional similarity region, and the far plume field. Separations between the regions, as in most naturally occuring phenomena, are not clear, as are the distinguishing characteristics of each region. The laminar two-dimensional boundary layer, or similarity region, which is the primary concern of this study, can be described by the similar solution of the laminar boundary layer theory. For the condition of two-dimensional convection above a line heat source located horizontally in a large fluid space, the primary variables describing the flow and the temperature are taken as indicated in Figure 1, where x and y are the vertical and horizontal coordinates with the origin at the heat source, and u and v are the velocity components in the x and y direction repectively.

The first step in the analysis of a combined convection and radiation heat transfer problem in the similarity region is the application of the conservation laws of mass, momentum and energy. The classical forms of these equations are well known and, therefore, are not considered here. Attention is focused on the equation of energy including the terms due to thermal radiation. The governing equations



(a) CASE I AND CASE II



(b) CASE III AND CASE IV

Fig. 1. Coordinate Systems

are based on the following assumptions: (1) steady state, (2) Newtonian fluid, (3) laminar flow, (4) incompressible fluid, (5) two dimensional flow, (6) continuous medium, (7) No-slip condition for the third and fourth cases.

The equations of conservation based on the above assumptions take the following forms:

Conservation of mass:

$$\frac{\partial u}{\partial x} + \frac{\partial v}{\partial y} = 0 \tag{2-1}$$

Conservation of momentum:

$$\rho\left(u\frac{\partial u}{\partial x} + v\frac{\partial u}{\partial y}\right) = -\frac{\partial P}{\partial x} - \rho g + \mu\frac{\partial^2 u}{\partial y^2} \tag{2-2}$$

Conservation of energy:

$$u\frac{\partial T}{\partial x} + v\frac{\partial T}{\partial y} = \frac{k}{\rho C_p}\left(\frac{\partial^2 T}{\partial y^2}\right) - \frac{1}{\rho C_p}\frac{\partial q_r}{\partial y} \tag{2-3}$$

In equation (2-3), the quantity q_r refers to the thermal radiation heat flux, and k is the thermal conductivity of the fluid. The scope of this study is restricted to laminar flow only. The properties of thermal conductivity, density and the other empirical constants are assumed to be constant in the boundary layer, and only the steady state condition is being considered. The dissipation effects are neglected because these effects are small when compared to the other mechanisms of the flow. Gebhart [16] in 1962 demonstrated that the effect of viscous dissipation in natural convection becomes important only when $g\beta/C_p > 10^{-4}$,

i.e., when the induced kinetic energy becomes appreciable compared to the amount of heat transfer. The quantity $g\beta/C_p$ remains in the range 10^{-7} - 10^{-4} for fluids as different as liquid sodium, mercury, gases at ordinary temperature, water and viscous silicons for the terretial level of gravity.

The pressure gradiant may be expressed as

$$\frac{\partial p}{\partial x} = -\rho_\infty g \tag{2-4}$$

which comes from Newton's second law of motion. The force may also be given in terms of temperature;

$$-\rho_\infty g = \beta g T_\infty \tag{2-5}$$

and

$$\rho = \beta T \tag{2-6}$$

where β is the volume expansion coefficient.

$$\beta = -\frac{1}{\rho}\left(\frac{\partial \rho}{\partial T}\right)_p \tag{2-7}$$

Thus, the momentum equation (2-2) becomes;

$$\rho\left(u\frac{\partial u}{\partial x} + v\frac{\partial v}{\partial y}\right) = \rho g \beta (T - T_\infty) + \mu\frac{\partial^2 u}{\partial y^2} \tag{2-8}$$

In the case of radiating media, the degree of absorbing radiation of the medium has an effect on radiation transport by the medium. The parameter associated with radiation transport of the media is the optical thickness of the medium k_λ which is defined as the dimensionless

quantity:

$$k_\lambda(S) = \int_0^S K_\lambda(S^*)\, dS^* \qquad (2\text{-}9)$$

where S^* is a dummy variable of integration, S is a coordinate along the path of radiation, and K_λ is the extinction coefficient of the fluid which is composed of two parts, absorption coefficient a_λ and scattering coefficient σ_λ:

$$K_\lambda = a_\lambda + \sigma_\lambda \qquad (2\text{-}10)$$

The quantity $k_\lambda(S)$ is the optical thickness or opacity of the layer of thickness S, and is a function of all the vaues of K_λ between 0 and S. Because K_λ is a fuction of the local parameters such as pressure, absolute temperature, and concentration of the fluid in mixture, the optical thickness becomes a function of all these conditions along the path between 0 and S. The optical thickness is a measure of the ability of a given path length of gas to attenuate radiation of a given wavelength. A large optical thickness means large attenuation. The quantity k_λ is a convenient dimensionless parameter that will occur in the solutions of radiative transfer problems.

For a gas that is of uniform composition and is at uniform temperature and pressure (a uniform gas) or for a gas with K_λ independent of the local parameters, equation (2-9) becomes:

$$k_\lambda = K_\lambda S \qquad (2\text{-}11)$$

The optical thickness then depends directly on the extinction coefficient and the thickness of the absorbing-scattering layer. By

introducing an extinction mean free path ℓ_m, which is inversely propotional to the extinction coefficient K_λ, one obtains from equation (2-11):

$$k_\lambda = S/\ell_m \tag{2-12}$$

Thus the optical thickness is the number of mean penetration distances.

If $k_\lambda >> 1$, the medium is optically thick; that is, the mean penetration distance is quite small compared to the characteristic dimension of the medium. For this condition a volume element within the fluid is only influenced by the surrounding neighboring elements. If $k_\lambda << 1$, the medium is optically thin and the mean penetration distance is much larger than the medium dimension. Radiation can pass entirely though the material without significant absorption, and each element within the medium interacts directly with the medium boundary. Radiation emitted within the material is not reabsorbed by the material; this condition is called negligible self-absorption.

If consideration is confined to an optically thick medium, the so-called Rosseland approximation of the radiation heat flux q_r may be employed. This approximation is given by the following expression;

$$q_r = -\frac{4\lambda^2\sigma}{3K}\frac{\partial T^4}{\partial y} \tag{2-13}$$

where K is absorbtivity of the medium, σ is the Stefan-Boltzman constant and λ is the wavelength of the emitted radiation.

Applying the Rosseland approximation into the energy equation, the equation (2-3) becomes;

$$u\frac{\partial T}{\partial x}+v\frac{\partial T}{\partial y}=\frac{k}{\rho C_p}\frac{\partial^2 T}{\partial y^2}+\frac{4\lambda^2\sigma}{3K\rho C_p}\frac{\partial^2 T^4}{\partial y^2} \qquad (2\text{-}14)$$

The thermal diffusivity, α, is expressed by the relation $\alpha=\frac{k}{\rho C_p}$. The effects of nonlinearity, which is apparent from the term T^4, can be linearized. The term T^4 may be expressed as a linear function of temperature by expanding T^4 about T_∞ in a Taylor series. Neglecting the higher order terms in the expansion, the linearized form can be expressed in the approximating expression as

$$T^4 \approx 4T_\infty T - 3T_\infty^4 \qquad (2\text{-}15)$$

Subsituting (2-15) into (2-14), the energy equation becomes

$$u\frac{\partial T}{\partial x}+v\frac{\partial T}{\partial y}=\alpha\frac{\partial^2 T}{\partial y^2}+\frac{16\lambda^2\sigma T_\infty^3}{3K\rho C_p}\frac{\partial^2 T}{\partial y^2} \qquad (2\text{-}16)$$

The Rosseland approximation leads to a considerable simplification in the expression for radiant flux. The integral representation is now replaced by a simple diffusion-type equation. The simplicity is, however, offset by its approximate nature and other disadvantages:

(i) The approximation is valid at points far (optically) from the bounding surface and only for intense absorption, i.e. when the fractional variation in temperature is small in a distance of one mean free path. The approximation breaks down in the vincinity of the surface, since it does not take into account the radiation leaving the surface; the presence of the surface in this limiting conduction region, changes the coefficient from 16/3 to 8/3 in equation (2-16).

(ii) The last term in equation (2-16) represents only the sum of the first two terms in the Taylor series expansion of the black-body

emissive power, and therefore in some physical problems the error in truncating the series could be appreciable.

In spite of these shortcomings the Rosseland approximation has been used with success in a variety of problems ranging from transport of radiation through gases at low density to the study of the effects of radiation on blast waves caused by nuclear explosions.

Sparrow and Cess[5] defined a dimensionless quantity, N, called the conduction-to-radiation parameter which depicts the relative contributions of conduction and radiation to the heat transfer process. This quantity is defined as

$$N = \frac{kK}{4\lambda^2 \sigma T_\infty^3} \tag{2-17}$$

Substituting (2-17) into (2-16), the energy equation becomes

$$u\frac{\partial T}{\partial x} + v\frac{\partial T}{\partial y} = \alpha\left(1 + \frac{4}{3N}\right)\frac{\partial^2 T}{\partial y^2} \tag{2-18}$$

The continuity, momentum and energy equations can be reduced to two ordinary differential equations with boundary conditions by introducing a similarity variable $\eta(x,y)$ and a stream function $\phi(x,y)$ as

$$\eta = \frac{y}{x}\sqrt[4]{\frac{Gr_x}{4}} \tag{2-19}$$

$$\xi = x \tag{2-20}$$

$$\psi = 4\nu\sqrt[4]{\frac{Gr_x}{4}}\, f(\eta) \tag{2-21}$$

The Grashof number for a Newtonian fluid is defined as

$$Gr_x = \frac{g\beta x^3 (T_o - T_\infty)}{\nu^2} \tag{2-22}$$

Gebhart et al.[1] suggested that the plume centerline temperature variation with x could be expressed as

$$T_o - T_\infty = Ax^n \tag{2-23}$$

It will be shown that this form of the centerline temperature distribution is an appropriate one for certain flow configurations, because n may be chosen so that necessary conditions on the heat flow convected thermal energy across horizontal planes are satisfied. The nondimensional temperature $\phi(\eta)$ is defined as

$$\phi(\eta) = \frac{T - T_\infty}{T_o - T_\infty} \tag{2-24}$$

so that the local temperature is

$$T - T_\infty = Ax^n \phi(\eta) \tag{2-25}$$

Defining

$$u = \frac{\partial \psi}{\partial y} \tag{2-26}$$

from the continuity equation (2-1)

$$v = -\frac{\partial \psi}{\partial x} \tag{2-27}$$

Substituting equations (2-24), (2-25), (2-26) into the momentum and energy equations, we obtain

$$\rho\left(\frac{\partial \psi}{\partial y}\frac{\partial^2 \psi}{\partial x \partial y} - \frac{\partial \psi}{\partial x}\frac{\partial^2 \psi}{\partial y^2}\right) = \rho g \beta (T_o - T_\infty)\phi(\eta) + \mu \frac{\partial^3 \psi}{\partial y^3} \tag{2-28}$$

$$\frac{\partial \psi}{\partial y}\frac{\partial}{\partial x}\{x^n \phi(\eta)\} - \frac{\partial \psi}{\partial x}\frac{\partial}{\partial y}\{x^n \phi(\eta)\} = \frac{k}{\rho C_p}\frac{\partial^2}{\partial y^2}\{x^n \phi(\eta)\} \qquad (2\text{-}29)$$

Substituting equation (2-22) into equations (2-19), (2-20), and (2-21) gives

$$\eta = \frac{y}{x}\left\{\frac{g\beta x^3(T_o - T_\infty)}{4\nu^2}\right\}^{\frac{1}{4}} = y x^{\frac{1}{4}(n-1)}\left(\frac{g\beta A}{4\nu^2}\right)^{\frac{1}{4}} \qquad (2\text{-}30)$$

$$\psi = 4\nu\left\{\frac{g\beta x^3(T_o - T_\infty)}{4\nu^2}\right\}^{\frac{1}{4}} f(\eta) = 4\nu x^{\frac{1}{4}(3+n)}\left(\frac{g\beta A}{4\nu^2}\right)^{\frac{1}{4}} f(\eta) \qquad (2\text{-}31)$$

Define a constant B as

$$B = \frac{g\beta A}{4\nu^2} \qquad (2\text{-}32)$$

Then equations (2-30) and (2-31) become

$$\eta = B^{\frac{1}{4}} y x^{\frac{1}{4}(n-1)} \qquad (2\text{-}33)$$

$$\psi = 4\nu B^{\frac{1}{4}} x^{\frac{1}{4}(n+3)} f(\eta) \qquad (2\text{-}34)$$

With these similarity variables defined in equations (2-20), (2-33), and (2-34), further mathematical manipulation results in the following set of ordinary differential equations for the momentum and energy equations.

Conservation of momentum:

$$f''' - (2n+2)f'^2 + (3+n)ff'' + \phi = 0 \qquad (2\text{-}35)$$

Conservation of energy:

$$\phi'' + P_r\{(n+3)f\phi' - 4nf'\phi\}/(1 + 4/3N) = 0 \qquad (2\text{-}36)$$

If the conduction-to-radiation parameter N becomes very large, the thermal radiation effect can be negligible. In this case N can be assumed infinite and the energy equation (2-36) becomes

$$\phi'' + Pr\{(n+3)f\phi' - 4nf'\phi\} = 0 \qquad (2\text{-}37)$$

This equation is exactly the same as the equation for a steady laminar natural convection plumes above a horizontal line heat source without thermal radiation effects, which was already derived by Gebhart et al [1].

Up to this point the analysis has been general, i.e, both equations (2-35) and (2-36) are applicable not only to plumes arising from a horizontal line source but also to the boundary layer flow over a vertical plate. Proper boundary conditions specify the particular case. Boundary conditions along with the values of A and n in equation (2-23) are determined for a plume by satisfying the necessary conditions on a plume flow resulting from a line source. The energy convected across any horizontal plane at x in the plume is

$$Q = \rho C_p \int_{-\infty}^{\infty} (T - T_\infty)\, u\, dy \qquad (2\text{-}38)$$

In terms of the similarity variables, Q becomes

$$Q = \rho C_p \int_{-\infty}^{\infty} A x^n \phi(\eta) \frac{\partial \psi}{\partial y}\, dy$$

$$= \rho C_p A x^n \int_{-\infty}^{\infty} \phi(\eta) B^{\frac{1}{4}}(4\nu)\, \xi^{\frac{1}{4}(n+1)} \frac{\partial f}{\partial \eta} B^{-\frac{1}{4}} x^{\frac{1}{4}(1-n)}\, d\eta$$

$$= 4\nu\rho C_p A B^{\frac{1}{4}} x^{\frac{1}{4}(5n+3)} \int_{-\infty}^{\infty} \phi(\eta) f'(\eta)\, d\eta \qquad (2\text{-}39)$$

Since Q is not a function of x (the only heat addition is due to the line source, there being no other sources), the value of n is found to be

$$n = -\frac{3}{5} \qquad (2\text{-}40)$$

The above result is also valid for natural convection flow over a vertical adiabatic surface with a heat source concentrated at the leading edge. With this value for n, equations (2-31), (2-32) become

Conservation of momentum :

$$f''' + \frac{12}{5} f f'' - \frac{4}{5} f'^2 + \phi = 0 \qquad (2\text{-}41)$$

Conservation of energy :

$$\phi'' + \frac{12}{5} Pr (f\phi)' / \left(1 + \frac{4}{3N}\right) = 0 \qquad (2\text{-}42)$$

B. BOUNDARY CONDITIONS

As shown in Figure 1, the fluid is moving up by means of natural convection with or without thermal radiation effects. If there is a plate above the line heat source, the plate should be impermeable and adiabatic. In this case the no slip condition is also assumed on its surface. The flow is assumed to be fully developed inside the boundary layer and no flow exists outside the boundary layer. The temperature

outside the boundary layer is defined as a constant bulk temperature T_∞. The above conditions provide the following boundary conditions;

For the first and second cases (see Figure 1(a)) :

$$U(X,0)=0 \tag{2-43}$$

$$\left.\frac{\partial u}{\partial y}\right|_{y=0}=0 \tag{2-44}$$

$$T(X,0)=0 \tag{2-45}$$

$$\left.\frac{\partial T}{\partial y}\right|_{y=0}=0 \tag{2-46}$$

$$\lim_{y\to\infty} u(X,y)=0 \tag{2-47}$$

$$\lim_{y\to\infty} T(X,y)=T_\infty \tag{2-48}$$

For the third and fourth cases (see Figure 1(b)):

$$u(X,0)=0 \tag{2-49}$$

$$U(X,0)=0 \tag{2-50}$$

$$T(X,0)=0 \tag{2-51}$$

$$\left.\frac{\partial T}{\partial y}\right|_{y=0}=0 \tag{2-52}$$

$$\lim_{y\to\infty} u(x,y)=0 \tag{2-53}$$

$$\lim_{y\to\infty} T(x,y)=0 \tag{2-54}$$

The dimensionless boundary conditions are obtained by applying equations (2-19), (2-20), (2-21), and (2-24) to the boundary conditions described above. The transformed dimensionless boundary equations are shown below.

For the first and second cases:

$$f(0)=0 \tag{2-55}$$

$$f''(0)=0 \tag{2-56}$$

$$\lim_{\eta\to\infty} f'(\eta)=0 \tag{2-57}$$

$$\phi(0)=1 \tag{2-58}$$

$$\phi'(0)=0 \tag{2-59}$$

$$\lim_{\eta\to\infty} \phi(\eta)=0 \tag{2-60}$$

For the third and fourth cases:

$$f(0)=0 \tag{2-61}$$

$$f'(0) = 0 \tag{2-62}$$

$$\lim_{\eta \to \infty} f'(\eta) = 0 \tag{2-63}$$

$$\phi(0) = 1 \tag{2-64}$$

$$\phi'(0) = 0 \tag{2-65}$$

$$\lim_{\eta \to \infty} \phi(\eta) = 0 \tag{2-66}$$

CHAPTER III

ANALYSIS OF THE SIMILARITY SOLUTION

A. SATISFACTION OF THE ASYMPTOTIC BOUNDARY CONDITIONS.

The momentum and energy equations derived in the previous chapter can not be sloved analytically. Furthermore, there are not enough conditions specified to determine all the constants of integration even if one could find a value $f(\eta)$ and $\phi(\eta)$ in an analytical form. For the numerical calculation of the ordinary differential equations, a complete specification of the boundary conditions is required. Constraints for f, f' and f" are required for the third order differntial equation in all cases. Also, the equation for ϕ is of the second order, which requires constraints for ϕ and ϕ'. At $\eta \to \infty$, the requirement that f'=0 due to its asymptotic approach automatically requires f"=0, and f'=0 implies that f must approach some constant value.

For the first and second cases, ϕ', f, f" are specified as 0, 0 and 0 at η=0. But no boundary conditions are given for f' and ϕ at η=0. No conditions are given for f' and ϕ at η=0. Therefore, this difficulty should be overcome.

The numerical integration of the ordinary differential equations of boundary-layer theory involves the satisfaction of asymptotic boundary conditions; that is, some boundary conditions are specified at the initial point or wall, and others are specified as limits that must be approached at large values of the independent variable corresponding to

the edge of the boundary layer, and it is necessary to specify as many additional conditions at the wall as there are conditions to be satisfied at the edge of the boundary layer. These additional initial conditions have to be varied in order to satisfy the conditions at the edge of the boundary layer. All methods that have been used to find the proper initial conditions rely on the fact that, for large values of the independent variable, the integrals of the differential equations depend on the initial conditions. One method that has been used to find the proper initial conditions, called the initial-value method, is that of obtaining integrals of the differential equations with guessed initial conditions; that is, an attempt is made to integrate the differential equations to the edge of the boundary layer. If this can be accomplished, corrections are made for the initial guesses by the Newton-Raphson method, and the process is repeated until a convergence is achieved.

In order to carry out this iteration, additional differential equations have to be integrated. The additional differential equations are obtained by differntiating the terms of the original differential equation with respect to the initial conditions. The integrals of these additional differential equations, henceforth referred to perturbation equations, give the rate of change of the integrals of the original differential equation with respect to the initial conditions.

Another method that has been used, called quasilinearization, is similar in principle to the initial-value method, except that the original differntial equations are linearized. The resulting linear

differntial equations for the current approximation are inhomogeneous since they also contain the previous approximation as members.

The integrals of the perturbation equations of the initial-value method correspond to a complementary solution of the linear differential equations of the quasilinearization method. In application, the two methods are different in that, in the quasilinearization method, the complementary solutions are used to obtain solutions to the inhomogeneous linear differential equations, whereas in the initial-value method, the integrals of the perturbation equations are used to adjust the starting values at the initial point. A disadvantage associated with the quasilinearization method is that functions representing the previous approximation have to be stored in order to construct the current approximation. Furthermore, the solution of the inhomogeneous equation obtained by combining complementary solutions and a particular integral is usually not well determined except near the orgin or initial point. The solutions of the perturbation equations, however, can be used to determine the proper initial conditions closely. This is the procedure that is followed in the initial-value method. Both methods have been used to obtain solutions of the boundary-layer equations. Neither of these methods, however, has solved the problem of when to stop the integration. since one boundary condition is specified as a limit that must be approached at large values of the independent variable, the integration should be stopped at a value of the independent variable that is sufficiently large so that the various functions are approaching their asymptotic values. This value of the

independent variable could properly be called the edge of the boundary layer. In the various methods used to solve this problem, this value of the independent variable must be guessed beforehand. If the guessd value is too samll, the integrals of the differential equation may not be able to satisfy the imposed conditions; or, there may be more than one value of an initial condition that leads to integrals of the differntrial equations that satisfy the imposed boundary conditions.

If the guessed value is too large, it is possible that the integrals of the equations will diverge, or that convergence to a solution is extremely slow.

In an effort to adapt the initial-value method to the solution of differential equations with asymptotic boundary conditions, a method was developed to eliminate the problem of when to stop the integration. This method of solution is capable of satisfying the boundary conditions at the edge of the boundary layer correctly; that is, the boundary values are approached asymptotically. This is accomplished by choosing the additional initial conditions so that the mean square error between the computed variables and the asymptotic values is minimized. The proposed method of solution is based on a least-squares convergence criterion in which the edge of the boundary layer is approached in steps. The convergence rate to a solution is rapid, and convergence appears to be insensitive to the initial guesses of the initial conditions. Use of a least-squares convergence criterion leads to the unique solution even in the case of retarded main stream flows. By using this method of solution it is feasible to obtain directly, for

those differential equations which contain a parameter, the relation between the properties of the solutions and the values of the parameter.

An algorithm by Nachtsheum and Swigert [6] is employed to solve ordinary differential equations in this research. Since there are two asymptotic boundary conditions to satisfy, two additional initial conditions on the wall will generally have to be specified. But this problem needs only one additional initial condition of temperature distribution on the wall because there is no heat transfer at $\eta = 0$ (i.e., $\phi'(0) = 0$).

Therefore, the guessed values of $z = f'(0)$ for the first and second cases and $z = f''(0)$ for the third and fourth cases are sought to satisfy simultaneously the nonlinear equations.

$$\phi_{edge}\{f''(0)\} = 0 \tag{3-1}$$

$$f'_{edge}\{f''(0)\} = 0 \tag{3-2}$$

where $f'_{edge} = f'(\eta_{edge})$.

The necessary first corrections to a first approximation z comes from a solution of the linear equations;

$$0 = f' + f'_z \Delta Z \tag{3-3}$$

and

$$0 = \phi + \phi_z \Delta Z \tag{3-4}$$

at $\eta = \eta_{edge}$, where $f'_z = \frac{\partial f'}{\partial Z}$ etc. However, in order to satisfy the

asymptotic boundary conditions, the preceding equations must be supplemented by

$$0 = f'' + f_z'' \Delta Z \tag{3-5}$$

and

$$0 = \phi' + \phi_z' \Delta Z \tag{3-6}$$

and Δz must be found such that the sum of squares of the errors in the preceding four equations be a minimum. The relations in equations (3-3), (3-4), (3-5), and (3-6) can never be absolutely satisfied due to the mathematical limitations involved in actually reaching infinity. They can be satisfied to some desired degree of accuracy such that

$$S_1 = f' + f_z' \Delta Z \tag{3-7}$$

$$S_2 = \phi + \phi_z \Delta Z \tag{3-8}$$

$$S_3 = f'' + f_z'' \Delta Z \tag{3-9}$$

$$S_4 = \phi' + \phi_z' \Delta Z \tag{3-10}$$

at $\eta = \eta_{edge}$ where S_1 , S_2 , S_3 and S_4 are values arbitrary close to zero. A least square solution for z can be obtained for the above equations which will make the sum $S_1^2 + S_2^2 + S_3^2 + S_4^2$ as small as required. This can be accomplished by differentiating $S_1^2 + S_2^2 + S_3^2 + S_4^2$ with respect to Δz and equating the result to zero. This procedure can be

carried out as follows.

$$S_1^2+S_2^2+S_3^2+S_4^2 = f'^2+\phi^2+f''^2+\phi'^2$$

$$+2\Delta z(f'f_z'+\phi\phi_z+\phi'\phi_z'+f''f_z'') + \Delta z^2(f_z'^2+\phi_z^2+f_z''^2+\phi_z'^2) \qquad (3\text{-}11)$$

$\frac{\partial}{\partial(\Delta z)}(S_1^2 +S_2^2 +S_3^2 +S_4^2)= 0$ gives;

$$\Delta z = -\frac{f'f_z'+\phi\phi_z+ff_z''+\phi'\phi_z'}{f_z'^2+\phi_z^2+f_z''^2+\phi_z'^2} \qquad (3\text{-}12)$$

The value of z that gives $\Delta z=0$ corresponds to the minimum with respect to z of the quantity

$$E = f'^2+\phi^2+f''^2+\phi'^2 \qquad (3\text{-}13)$$

at $\eta = \eta_{edge}$. The partial derivatives with respect to that appear in equation (3-12) are obtained by differentiating the terms in the momentum and energy equations appropriately with respect to z. The perturbation differential equations for the z derivatives are

(i) For the first and third cases:

$$f_z''' = -\frac{12}{5}(f_z f'' + f f_z'') + \frac{8}{5} f f_z - \phi_z \qquad (3\text{-}14)$$

$$\phi_z'' = -\frac{12}{5} Pr(f_z'\phi + f'\phi_z + f_z\phi' + f\phi_z') \qquad (3\text{-}15)$$

(ii) For the second and fourth cases:

$$f'''_z = -\frac{12}{5}(f_z f'' + f f''_z) + \frac{8}{5} f' f_z - \phi_z \qquad (3\text{-}16)$$

$$\phi''_z = -\frac{12}{5} Pr\,(f'_z \phi + f' \phi_z + f_z \phi' + f \phi'_z)/(1 + \frac{4}{3N}) \qquad (3\text{-}17)$$

The boundary conditions, equations (2-20) through (2-66), and the starting conditions for the pertubation equation can be derived from these as

(i) For the first and second cases:

$$f(0) = 0 \quad , \quad f_z(0) = 0 \qquad (3\text{-}18)$$

$$f'(0) = z \quad , \quad f'_z(0) = 1 \qquad (3\text{-}19)$$

$$f''(0) = 0 \quad , \quad f''_z(0) = 0 \qquad (3\text{-}20)$$

$$\phi(0) = 1 \quad , \quad \phi_z(0) = 0 \qquad (3\text{-}21)$$

$$\phi'(0) = 0 \quad , \quad \phi'_z(0) = 0 \qquad (3\text{-}22)$$

(ii) For the third and fourth cases:

$$f(0) = 0 \quad , \quad f_z(0) = 0 \qquad (3\text{-}23)$$

$$f'(0) = 0 \quad , \quad f'_z(0) = 0 \qquad (3\text{-}24)$$

$$f''(0)=z \quad , \quad f_z''(0)=1 \tag{3-25}$$

$$\phi(0)=1 \quad , \quad \phi_z(0)=0 \tag{3-26}$$

$$\phi'(0)=0 \quad , \quad \phi_z'(0)=0 \tag{3-27}$$

B. THE SOLUTION ALGORITHM

The Runge-Kutta algorithm is chosen to solve the differential equations since it is a stable algorithm and because the errors inherent in the numerical approximations using this scheme are generally well controlled. The algorithm uses Gill coefficients developed by Gill [15]. Gill coefficients allow better error control in moving from mode to mode across the solution domain. The algorithm has been incorporated into a computer program which is designed to compute the solution values for both the momentum and energy equations out to a point designated as η_{edge} where the corrections to the initial guesses for f"(0) are computed. The deviations of f' and ϕ from the asymptotic values are checked at $\eta = \eta_{edge}$, and if the error is larger than a prescribed value the magnitude of η_{edge} and the corrected initial guesses for f" or f' are used to resolve the equations until the boundary conditions and error limits are met. The initial guess used for η_{edge} is 6.0 which is increased by a small increment (0.1 or smaller depending upon DX in the program) until the convergence is achieved and the error requirement is met. The maximum error used in the analysis ranges from 0.05 to 0.0005. The values of the maximum error, DX and CPU time for different cases of

Prandtl Number (Pr), and the conduction-to-radiation parameter (N) are listed in Tables 1, 2, 3, and 4. The Digital Equipment Corporation (DEC) computer is used in this research. This computer is a symmetric multiprocessing (SMP) system model 1099 with two KL-10 central processing units (CPU's).

Figure 2 shows a schematic diagram and brief descriptions of the four cases investigated in this research.

Table 1. The Values of the Maximum Error, DX, and CPU Time for Case I.

Pr	N	EMAX	DX	CPU TIME
100.0	—	0.001	0.005	2:10.00
10.0	—	0.001	0.005	3:58.81
2.0	—	0.0005	0.05	4.39
1.0	—	0.0005	0.05	4.38
0.1	—	0.0005	0.05	22.23
0.01	—	0.01	0.05	3:51.09

Table 2. The Values of the Maximum Error, DX, and CPU Time for Case II.

Pr	N	EMAX	DX	CPU TIME
10.0	100.0	0.001	0.01	58.41
	1.0	0.001	0.01	56.86
	0.1	0.001	0.01	1:39.26
	0.1	0.001	0.01	13:33.03
1.0	100.0	0.001	0.05	4.22
	1.0	0.01	0.05	3.56
	0.1	0.0005	0.05	35.45
	0.01	0.01	0.05	2:54.05
0.1	100.0	0.0005	0.05	23.78
	1.0	0.001	0.05	52.05
	0.1	0.05	0.05	1:42.60

Table 3. The Value of he Maximum Error, DX, and CPU Time for Case III.

Pr	N	EMAX	DX	CPU TIME
100.0	—	0.001	0.005	17.44
10.0	—	0.001	0.005	46.70
2.0	—	0.0001	0.05	3.75
1.0	—	0.0001	0.05	3.75
1.0	—	0.0001	0.05	3.75
0.01	—	0.01	0.05	2:14.78

Table 4. The Values of the Maximum Error, DX, and CPU Time for Case IV.

Pr	N	EMAX	DX	CPU TIME
10.0	100.0	0.001	0.01	47.71
	1.0	0.001	0.01	1:23.34
	0.1	0.001	0.01	2:19.66
	0.01	0.001	0.01	15:09.57
1.0	100.0	0.001	0.05	3.46
	1.0	0.001	0.05	4.90
	0.1	0.001	0.05	34.25
	0.01	0.01	0.05	3:04.43
0.1	100.0	0.001	0.05	22.37
	1.0	0.001	0.05	50.58
	0.1	0.05	0.05	1:48.67

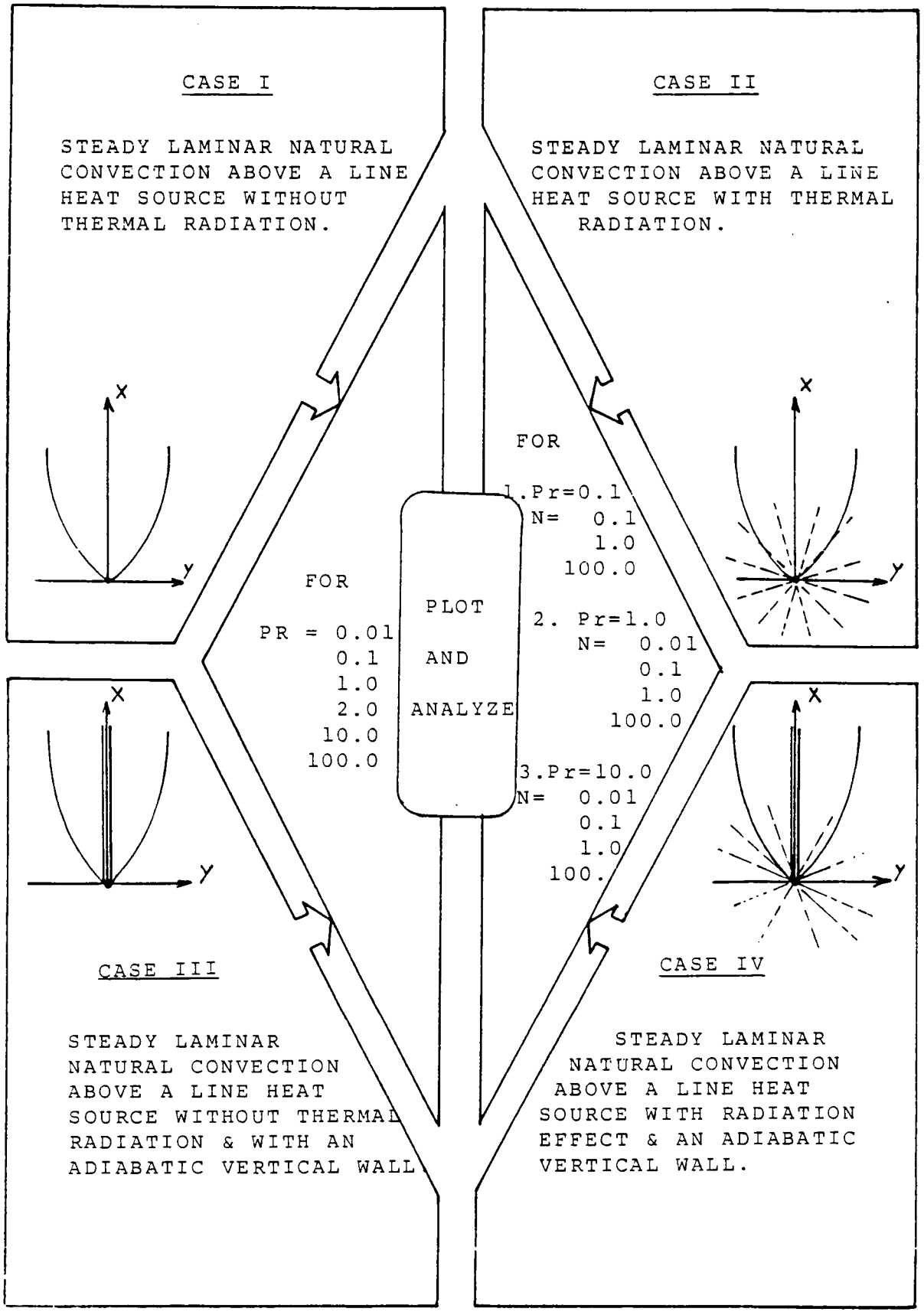


Fig. 2. Visualized Procedure of All Cases

C. RESULTS

Considering the natures of the Prandtl number, Pr, and the conduction-to-radiation parameter, N, the behaviors of velocity and temperature distributions can be predicted. Since the Prandtl number is defined as the ratio of the kinetic viscosity (ν) to the thermal diffusivity (α) as

$$Pr = \frac{\nu}{\alpha} \tag{3-28}$$

and represents the ratio of the diffusivity of momentum relative to the diffusivity of heat conduction, temperature and velocity profiles are identical when this dimensionless number is unity, which is approximately the case for most gases ($0.6 < Pr < 1.0$). The Prandtl number for liquids, however, varies widely, ranging from very large values for viscous oils to very small values (on the order of 0.01) for liquid metals which have high thermal conductivities. Therefore, the momentum boundary layer becomes larger than the thermal boundary layer if the Prandtl number is greater than 1. On the other hand, the thermal boundary layer becomes larger than the momentum boundary layer if the Prandtl number is less than 1. Figures 4 and 5* show these results. The results indicate that the momentum boundary layer reaches to $\eta = 3.0$ and the thermal boundary layer is about at $\eta = 0.7$ for Pr = 100.0. Where Pr is 1.0, both momentum and thermal boundary layer thicknesses become equal (approximately 3.9). As the Prandtl number becomes smaller (for

*Figures 3 through 23 may be found in Appendix A.

increasing while the Prandtl number and the conduction-to-radiation parameter are decreasing. This means that the shear stress on the vertical wall is larger in the radiation dominated natural convection flow or in the flow of high diffusivity of heat conduction.

Comparison of case I with case III (or case II with case IV) shows the influences of an adiabatic vertical wall above a line heat source. Figures 12, 14, 16, and 18 demonstrate the no slip condition for case III. Comparison of Figure 13 with Figure 5 shows the effect of the wall on the temperature distribution. For the first case, without an adiabatic vertical wall, the speed of the fluid is maximum at $\eta=0$. Therefore, the high speed makes rapid heat transfer near $\eta=0$ (compare Figure 23 with Figure 24 and see Table 7), and accelerates temperature distribution near the wall (compare Figure 5 with Figure 16). Figures 5 and 16 show that the thickness of thermal boundary layer increases as an adiabatic vertical wall which is placed above the line heat source. For example, the thermal boundary layer forms near $\eta=0.5$ for the first case (Figure 5) and near $\eta = 1.0$ for the second case (Figure 16) when the Prandtl number is 100.0. However, the existence of an adiabatic vertical wall above a line heat source has little effect on velocity profiles and thermal distributions far from the wall.

CHAPTER IV

CONCLUSIONS AND RECOMMENDATIONS

The results of this study provide a great deal of information which can be used to examine a laminar boundary layer flow under the influence of convection and radiation heat transfer. The problem studies the effects of Prandtl number and thermal radiation on laminar free convection above a line heat source with and without an adiabatic vertical wall. The study covers wide ranges of Prandtl numbers (from 0.01 to 100) and the conduction-to-radiation parameter (from 0.01 to 100). Solutions of the boudnary layer equations used in the analysis are found through the use of similarity transformations which produced ordinary differential forms of the momentum and energy equations. The solution of the energy equation is simplified by the use of the Rosseland approximation with linearized optically thick thermal radiation. The momentum and energy equations are numerically solved by using the modified Runge-Kutta method with Gill coefficients which provides corrections to initial guesses for the slope of the velocity and temperature profiles.

Study of the velocity and temperature profiles in the boundary layer provides the following conclusions:

1. The thicknesses of the momentum and thermal boundary layers of the fluid increase as he Prandtl number decreases, regardless of radiation effect.

2. If $Pr < 1$, the thermal boundary layer is larger than the velocity boundary layer, and if $Pr > 1$, the velocity boundary layer is larger than thermal boundary layer, regardless of thermal radiation .

3. The thicknesses of the momentum and thermal boundary layers and the maximum velocity of the fluid increase as the radiation heat transfer becomes more dominant ($N \rightarrow 0$). This leads to the conclusion that as the radiation heat transfer becomes dominant, the heat flux distribution becomes more evenly spread out in the fluid boundary layer.

4. Influence of an adiabatic vertical wall is evident in velocity and temperature distributions; that is, the velocity is zero on the wall due to the no slip condition, and the thicknesses of the thermal boundary layer of the fluid increases if the wall is placed above a line heat source.

Future research is expected to extend the study to include non-Newtonian fluids and different wall boundary conditions. Over two decades, considerable attention has been devoted to predicting the flow and heat transfer characteristics of a non-Newtonian fluids. The emergence of non-Newtonian fluid such as molten plastics, pulps, and emulsions as important raw materials and products in industrial processes has generated a considerable amount of interest in the behavior of such fluids. Therefore, it would be of interest to

investigate the same problem for the non-Newtonian fluids. However, some mathematical difficulties may be encountered in the process of obtaining the similarity variables. The procedure presented in this study may also be applicable to natural convection plumes over a vertical wall with uniform and non-uniform thermal boundary conditions in which temperature and velocity profiles may not develop similarly. It is also valuable to study thermal radiation effects in turbulent forced convection plume above horizontal line heat sources with and without an adiabatic vertical wall. For non-uniform thermal boundary conditions, one should investigate the method of solution of local similarity or nonsimilarity equations.

LIST OF REFERENCES

LIST OF REFERENCES

1. B. Gebhart, L. Pera and A. W. Schorr, "Steady laminar natural convection plumes above a horizontal line heat source," Int. J. Heat Mass Transfer 13, 161-171 (1970).

2. A. W. Schorr and B. Gebhart, "An experimental investigation of natural convection wakes above a line heat source," Int. J. Heat Mass Transfer 13,557-571 (1970).

3. T. Fujii, "Theory of steady laminar natural convection above a horizontal line heat source," Int. J. Heat Mass Transfer 6, 597-606 (1963).

4. White, H. M., Viscous Fluid Flows, 1st Ed., McGraw-Hill, New York (1974).

5. Sparrow, E. M., and Cess, R. D., Radiation Heat Transfer, 1st Ed.,Brooks/Cole Publishing, Belmont, Califonia (1965).

6. Nachtsheim, P. R., and Swigert, Paul, " Satisfaction of asymptotic boundary conditions in numerical solution of systems of non-linear equations of boundary layer type," NASA Technical Note D-3004, NASA (1965).

7. Kim, K. H., Ozisik, M. N., and Mulligan, J. C., "A non-similar solution of heat transfer in external non-Newtonian flow with thermal radiation," AIAA Paper No. 73-116 (1973).

8. Kim, K. H., Ozisik, M. N., " Application of normal-mode-expansion technique to absorbing, emitting and scattering point boundary layer flow," Development oin Theoretical and Applied Mechanics, Vol. 10, pp. 681, Proceedings of tenth southeastern conference on theoretical and applied mechanics (1980).

9. Viskata, R., and Grosh, R. J., "Boundary layer in thermal radiation absorbing and emitting media," Int. J. Heat Mass Transfer 5, 795-806 (1962).

10. D. B. Spalding and R. G. Cruddage, "theory of the steady laminar bouyant flow above a line heat source in a fluid of large Prandtl number and temperature-dependent viscosity," Int. J. Heat Mass Transfer 3, 55-59 (1961).

11. R. J. Forstrom and E. M. Sparrow, "Experiments on the buoyant plume above a heated horizontal wire," Int. J Heat Mass Transfer 10, 321-331 (1967).

12. M. J. Galuska and K. H. Kim, " Laminar natural convection heat transfer to non-Newtonian fluids with thermal radiation effects," Master thesis, The University of Tennessee, Knoxville (1982).

13. I. W. Diggs and K. H. Kim, " Curvature effects on heat transfer in the free jet boundary," AIAA Journal, Vol. 9, 1469-1471 (1982).

14. K. Brodowicz and W. T. Kierkus, " Experimental of larminar free convection flow in air above a horizontal wire with constant heat flux," Int. J. Heat Mass Transfer 9, 81-94 (1966).

15. S. Gill, " A process for the step-by-step integration of differential equations in an automatic digital computing machine," Proc. Cambridge Philos. Society 47, 96-108 (1950).

16. B. Gebhart, "Effect of viscous dissipation in natural convection," J. Fluid Mech. 14, 225-232 (1962).

17. R. B. Bird, W. E. Stewart, and E. N. Lightfoot, Transport Phenomena, Wiley, New York (1960).

18. Siegel, R., and Howell, J. R., Thermal radiation heat transfer, 2nd eds., McGraw-Hill, New York (1981).

APPENDIXES

APPENDIX A

ADDITIONAL FIGURES

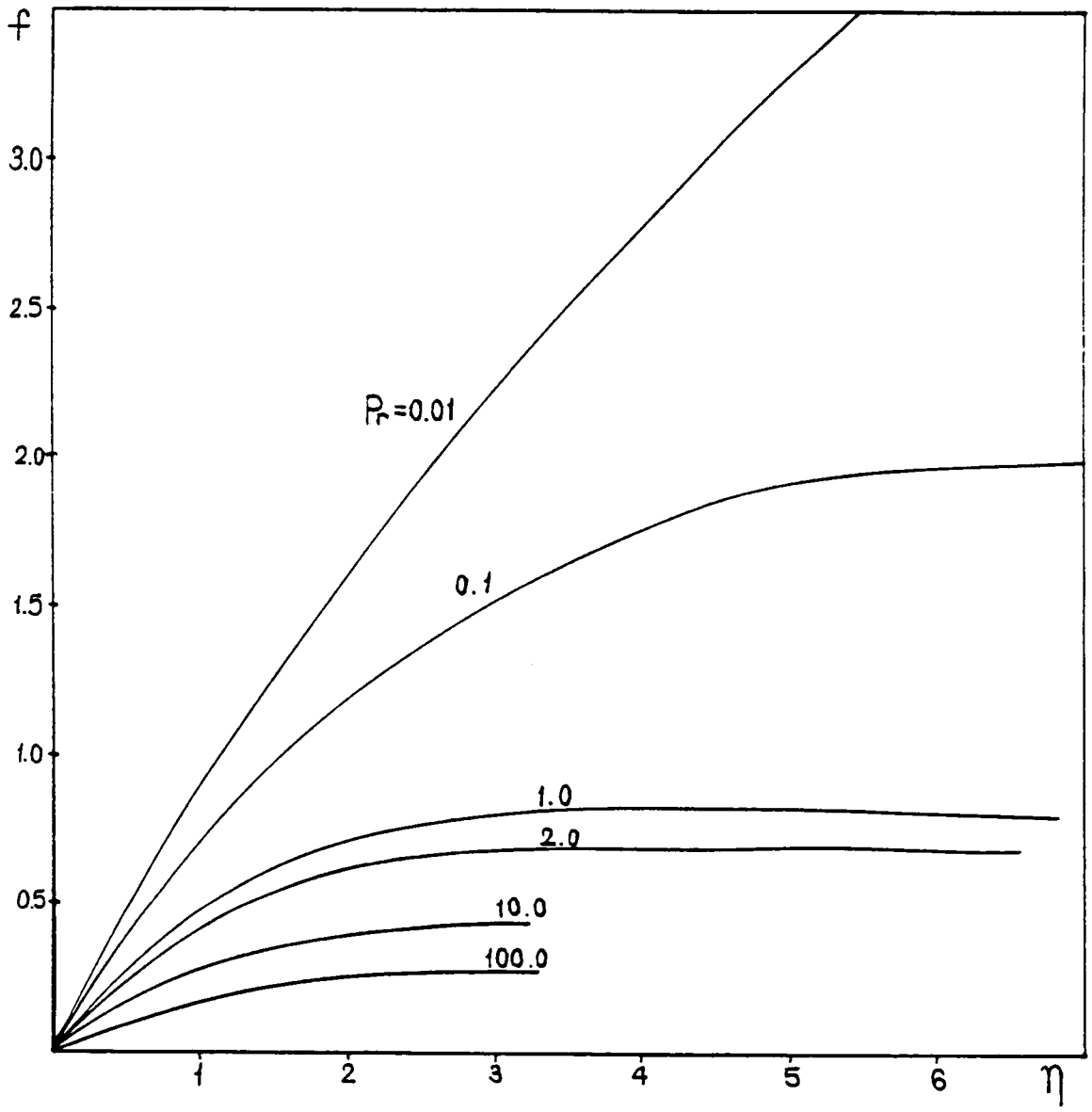


Fig. 3. Computed Value of f for Case I.

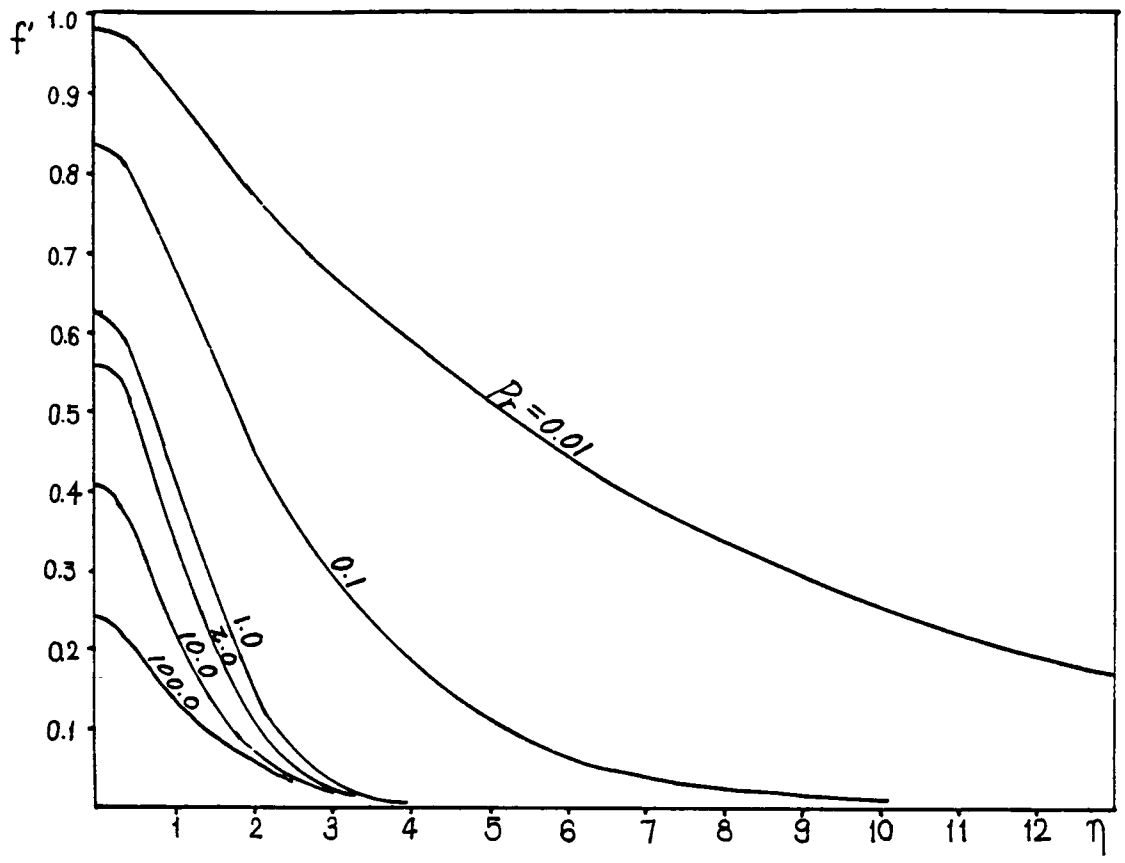


Fig. 4. Computed Velocity Profiles for Case I.

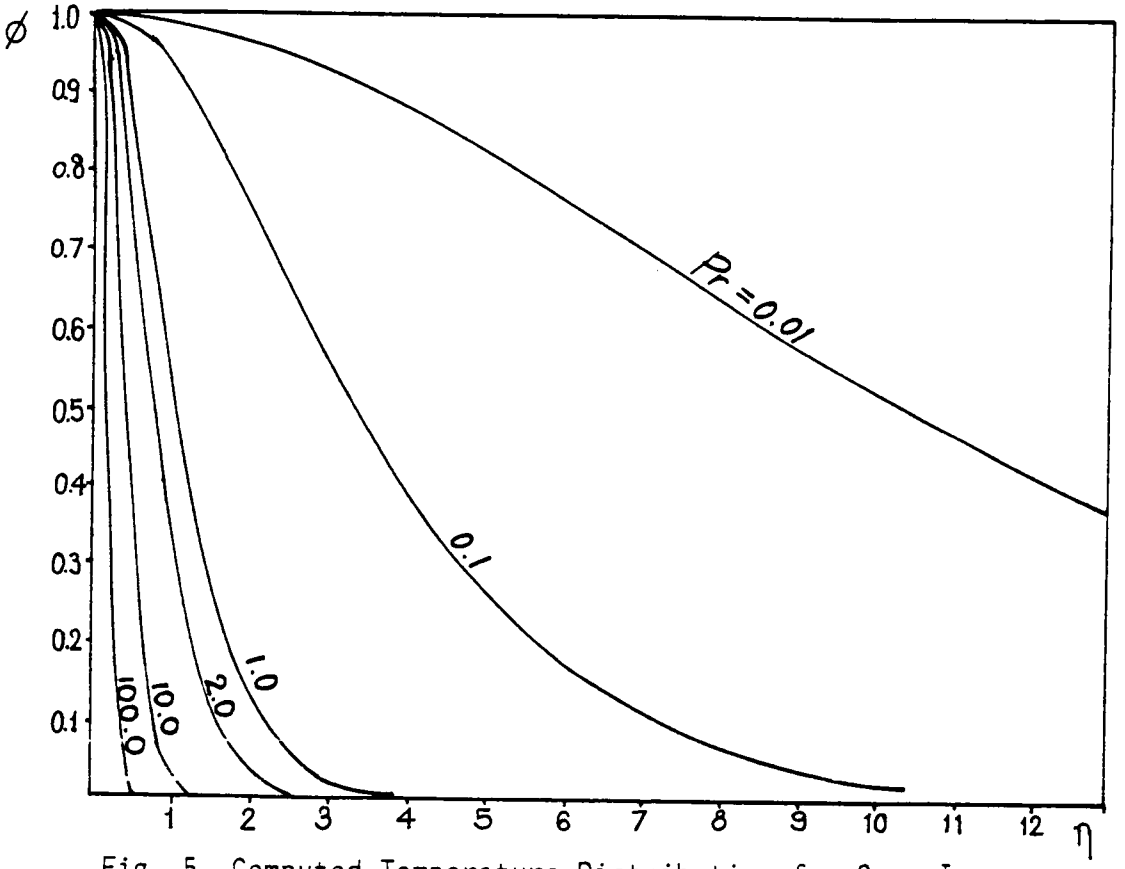


Fig. 5. Computed Temperature Distribution for Case I.

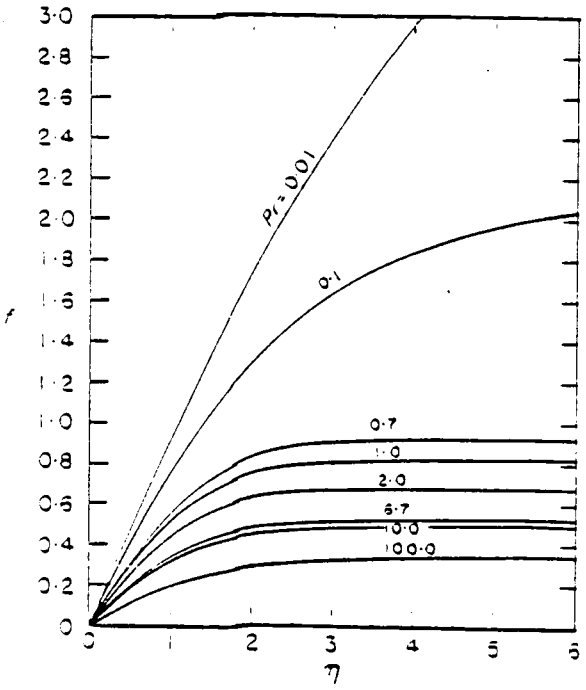


Fig. 6. Computed Value of f for a Range of Prandtl Numbers by Gebhart et al.

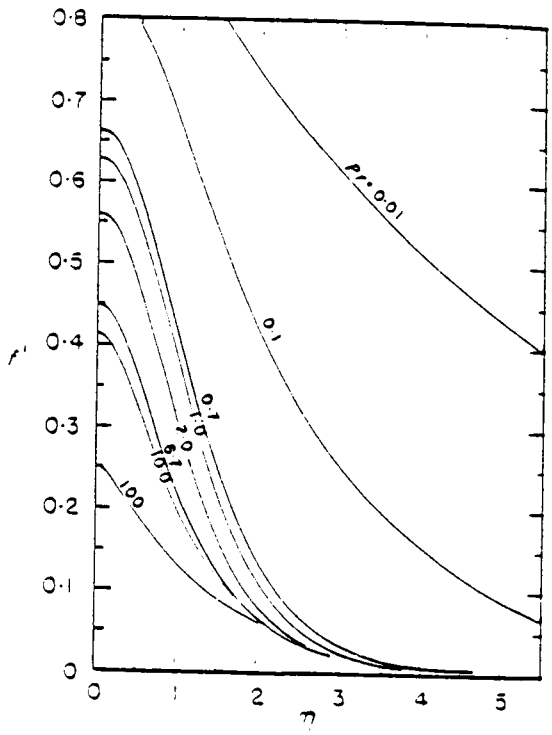


Fig. 7. Computed Value of Velocity Profiles for a Range of Prandtl Numbers by Gebhart et al.

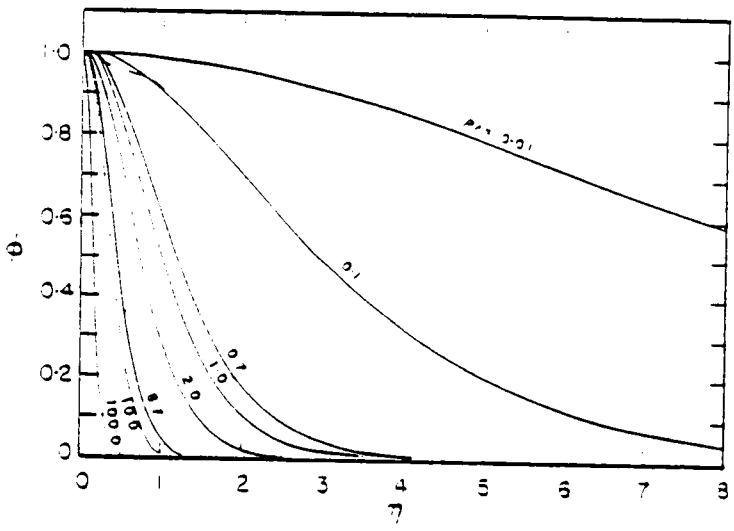


Fig. 8. Computed Temperature Distribution for a Range of Prandtl Numbers by Gebhart et al.

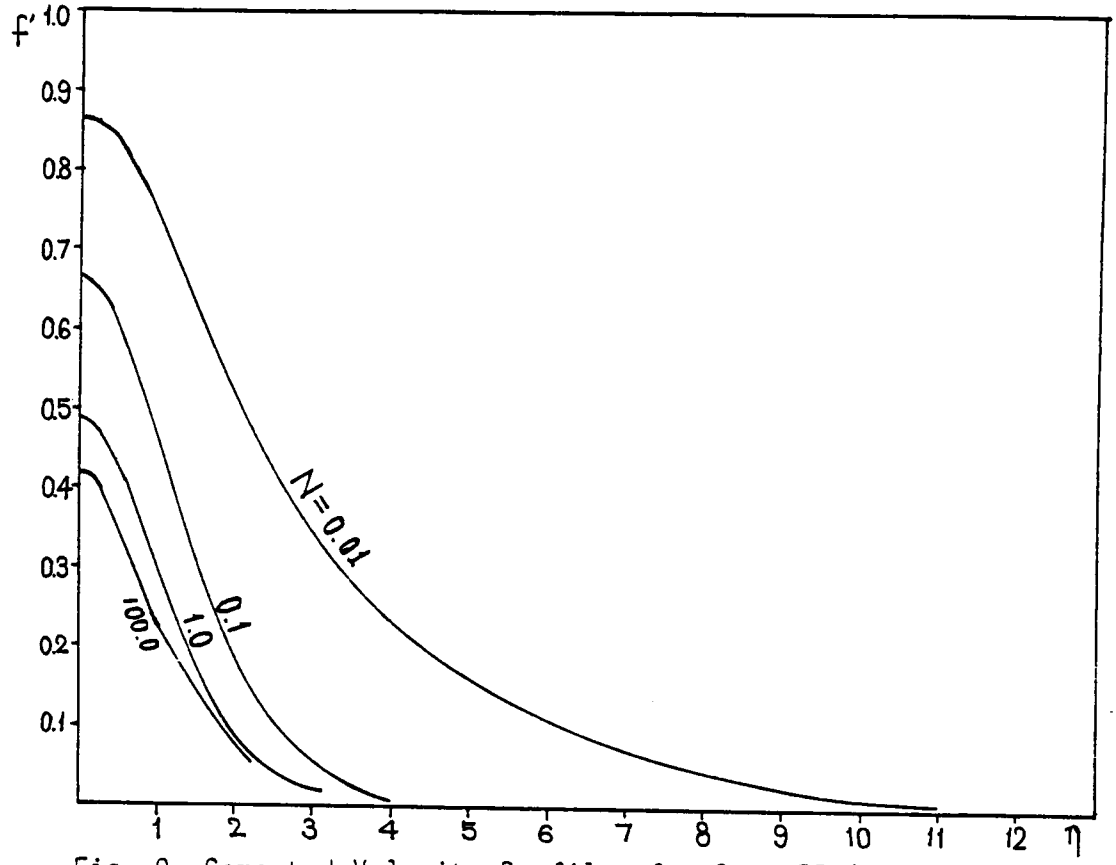


Fig. 9. Computed Velocity Profiles for Case II (Pr=10.0)

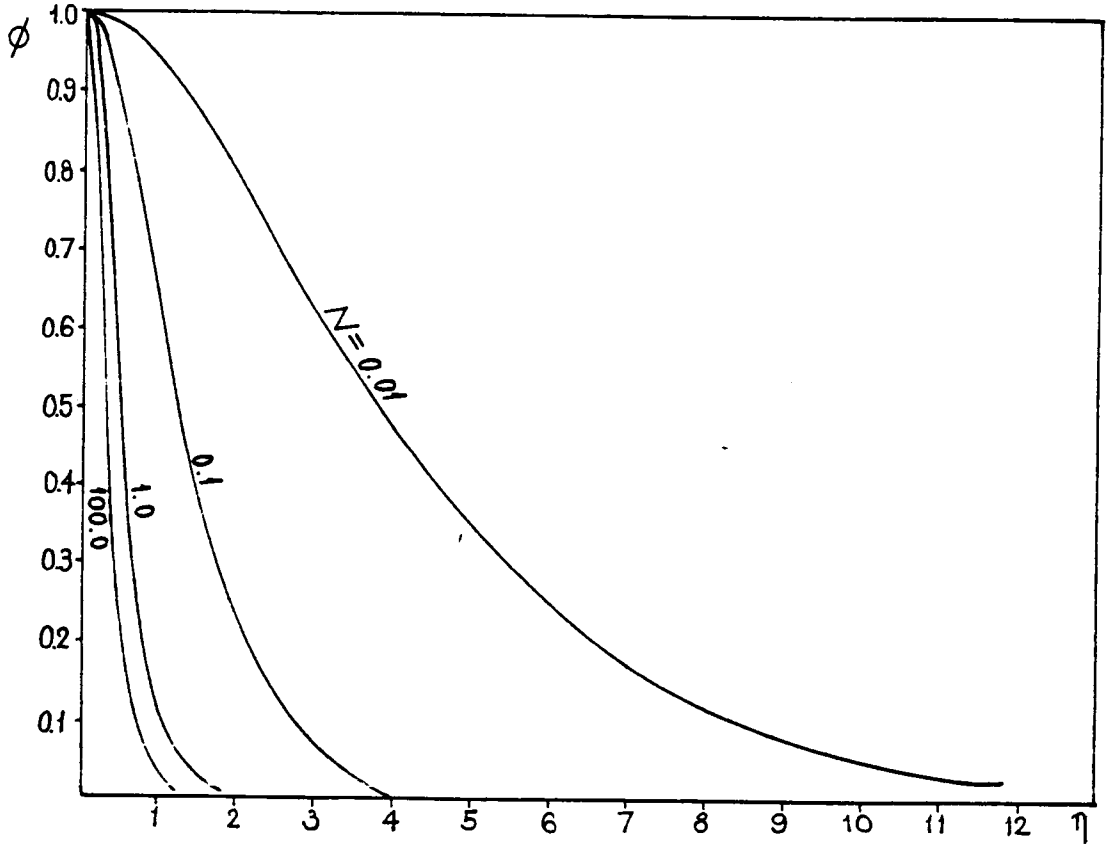


Fig. 10. Computed Temperature Distribution for Case II.(Pr=10.0)

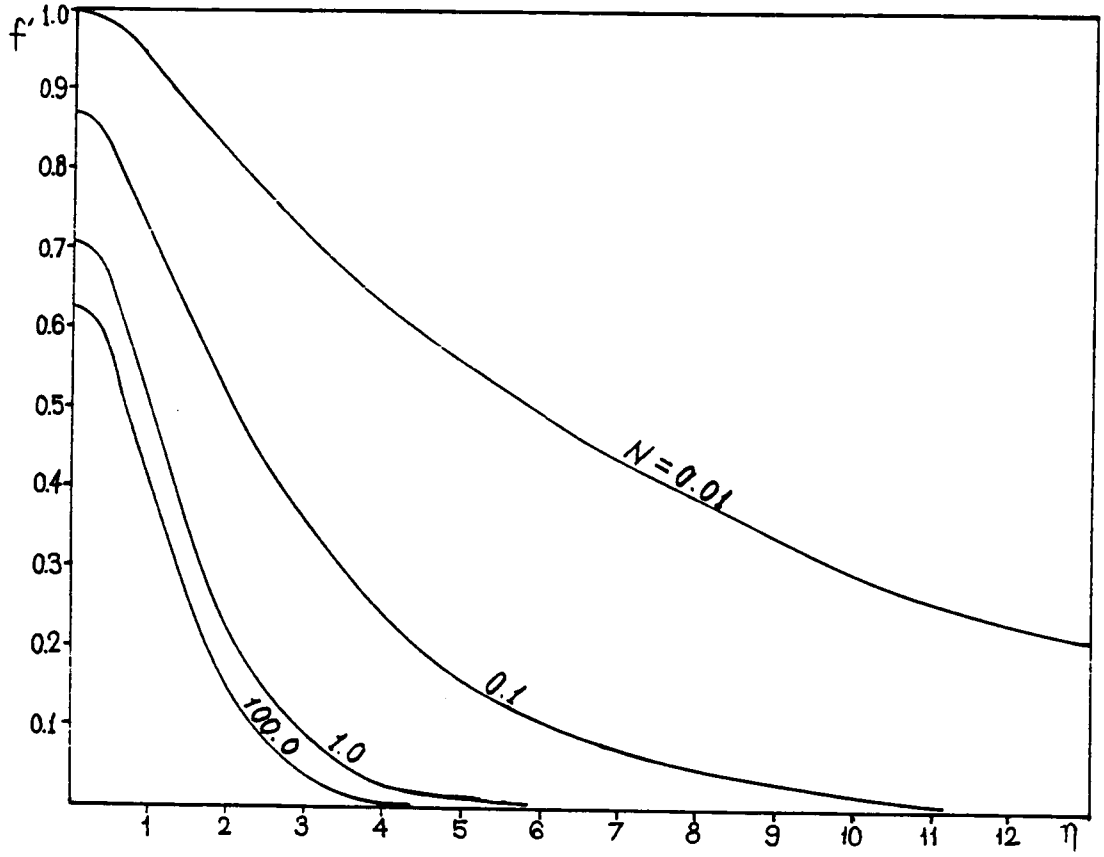


Fig. 11. Computed Velocity Profiles for Case II (Pr=1.0).

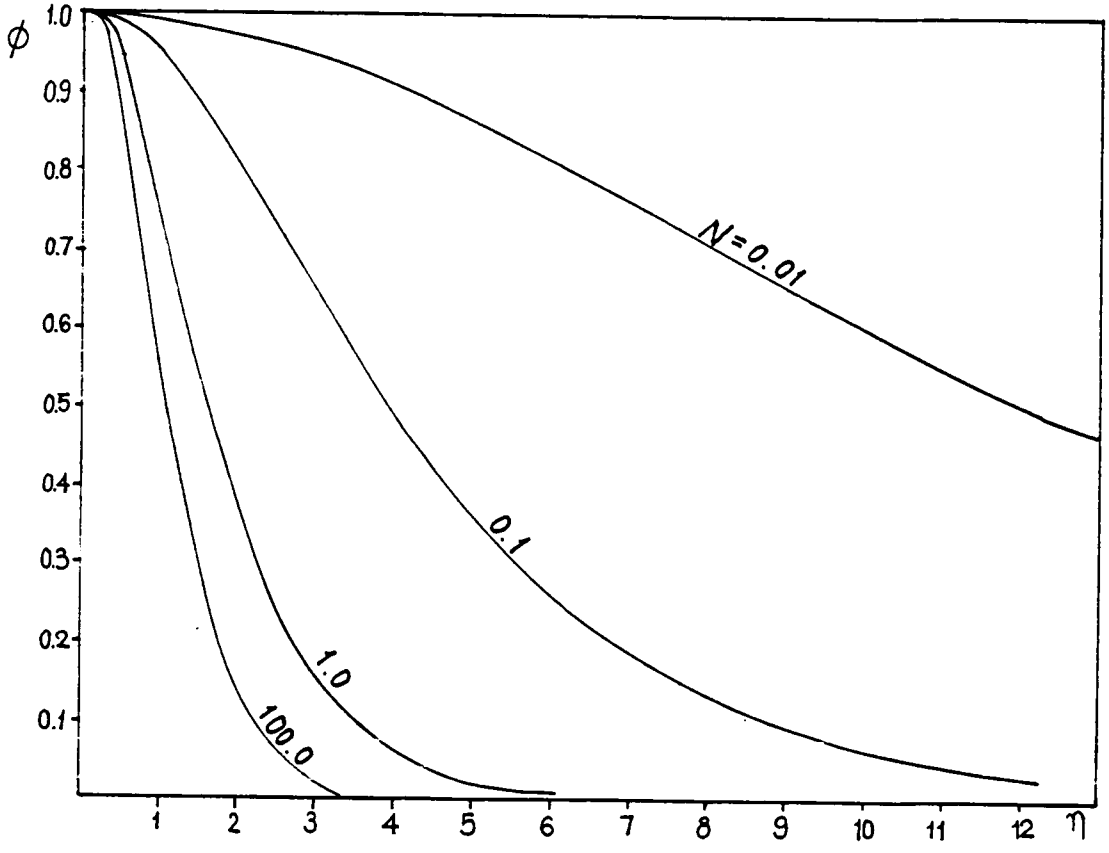


Fig. 12. Computed Temperature Distribution for Case II (Pr=1.0).

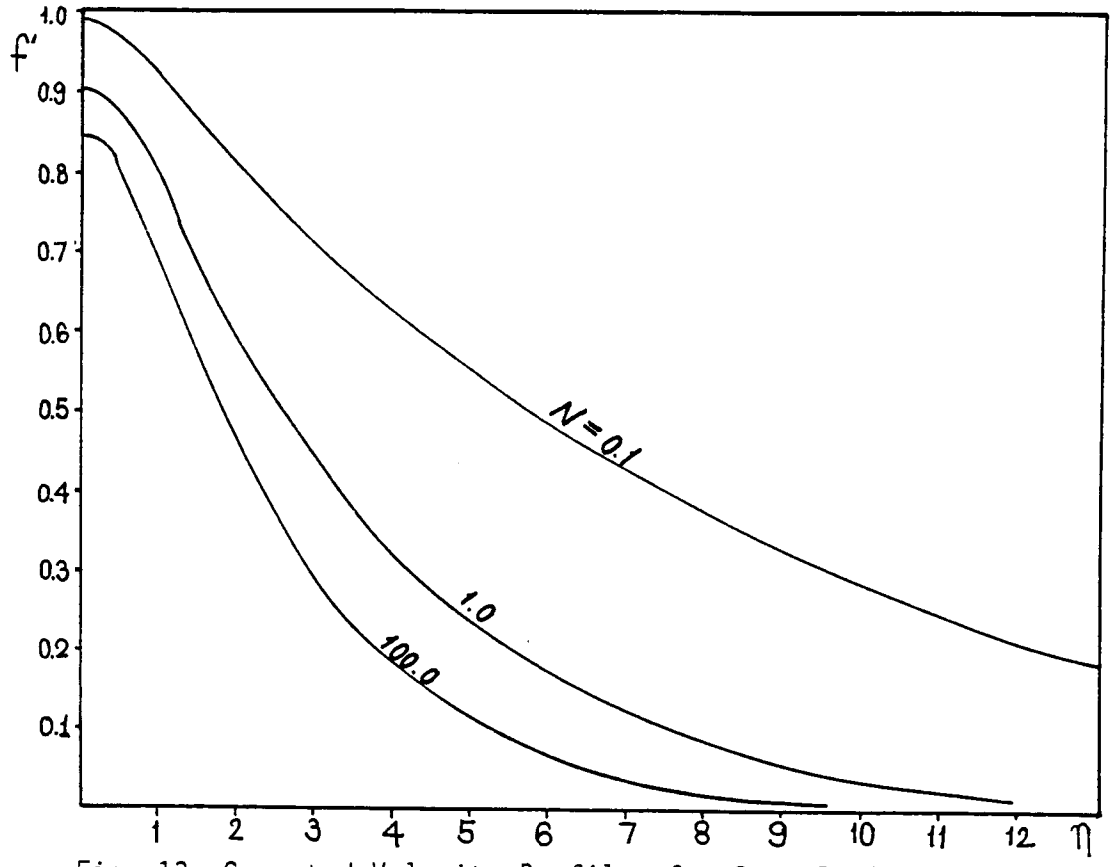


Fig. 13. Computed Velocity Profiles for Case II (Pr=0.1).

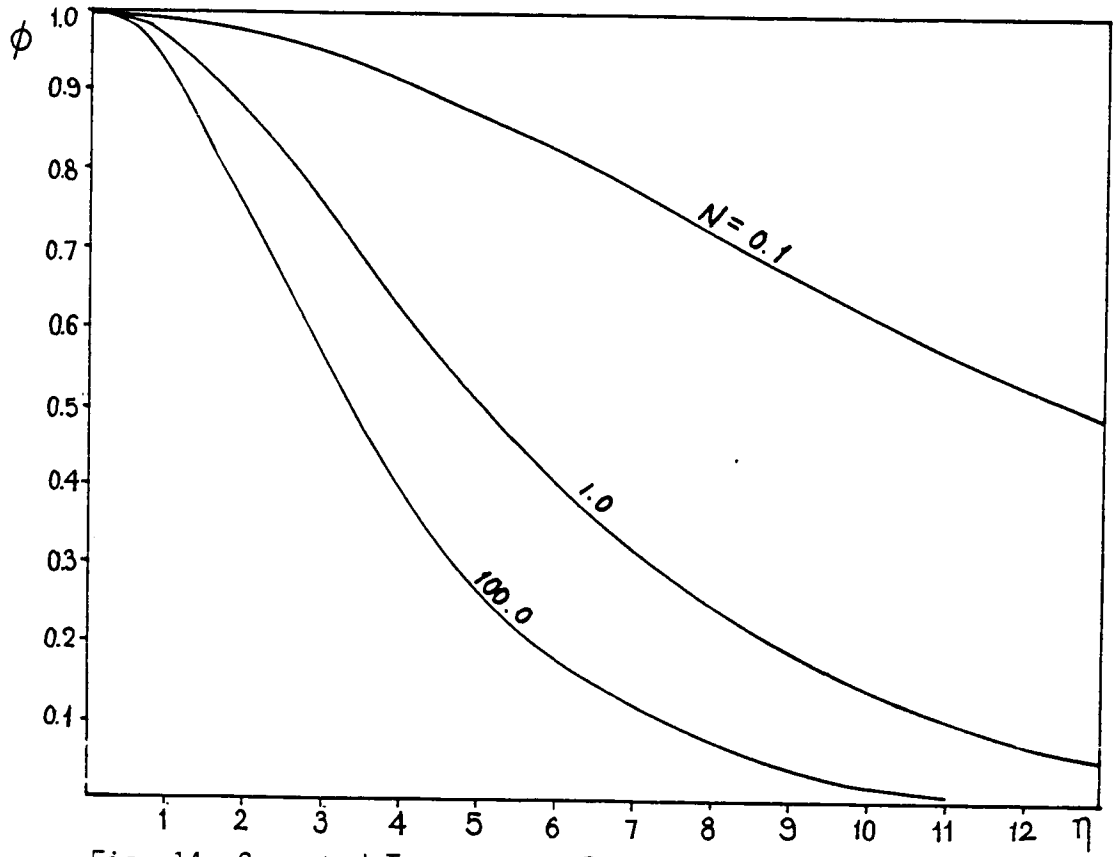


Fig. 14. Computed Temperature Distribution for Case II (Pr=0.1).

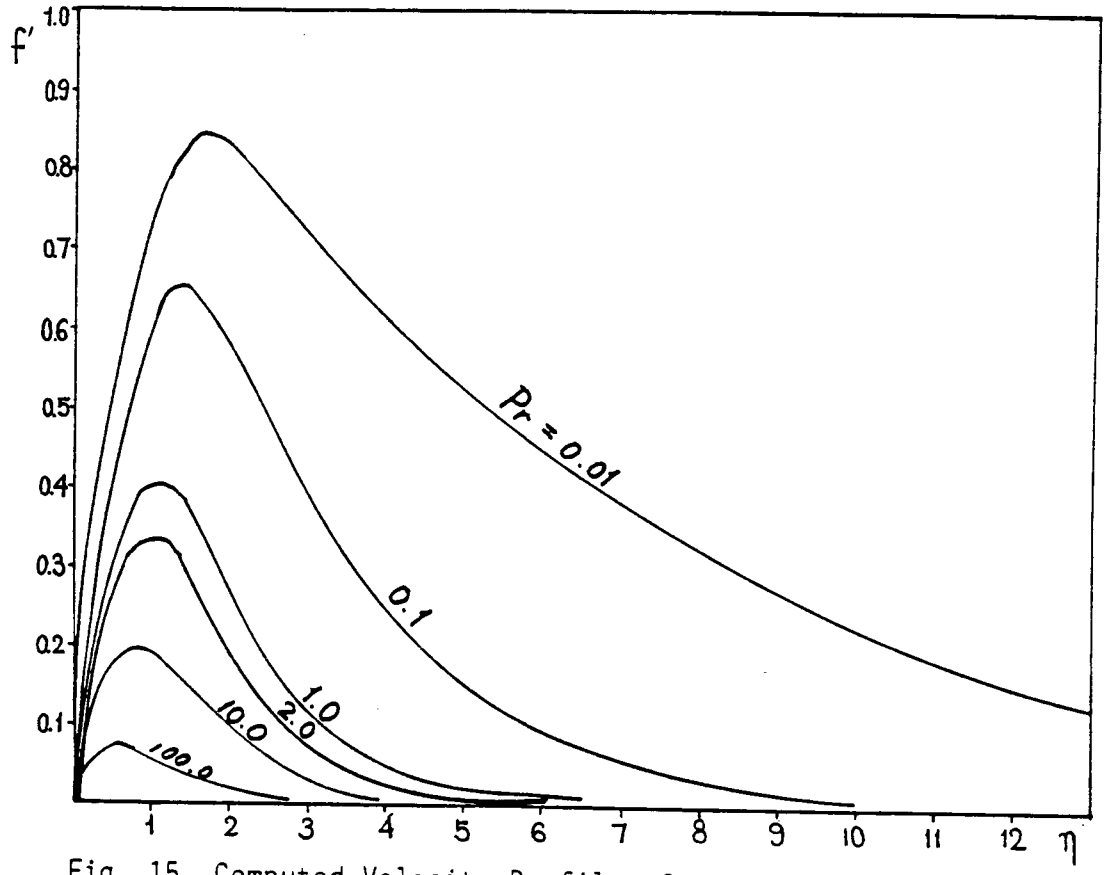


Fig. 15. Computed Velocity Profiles for Case III.

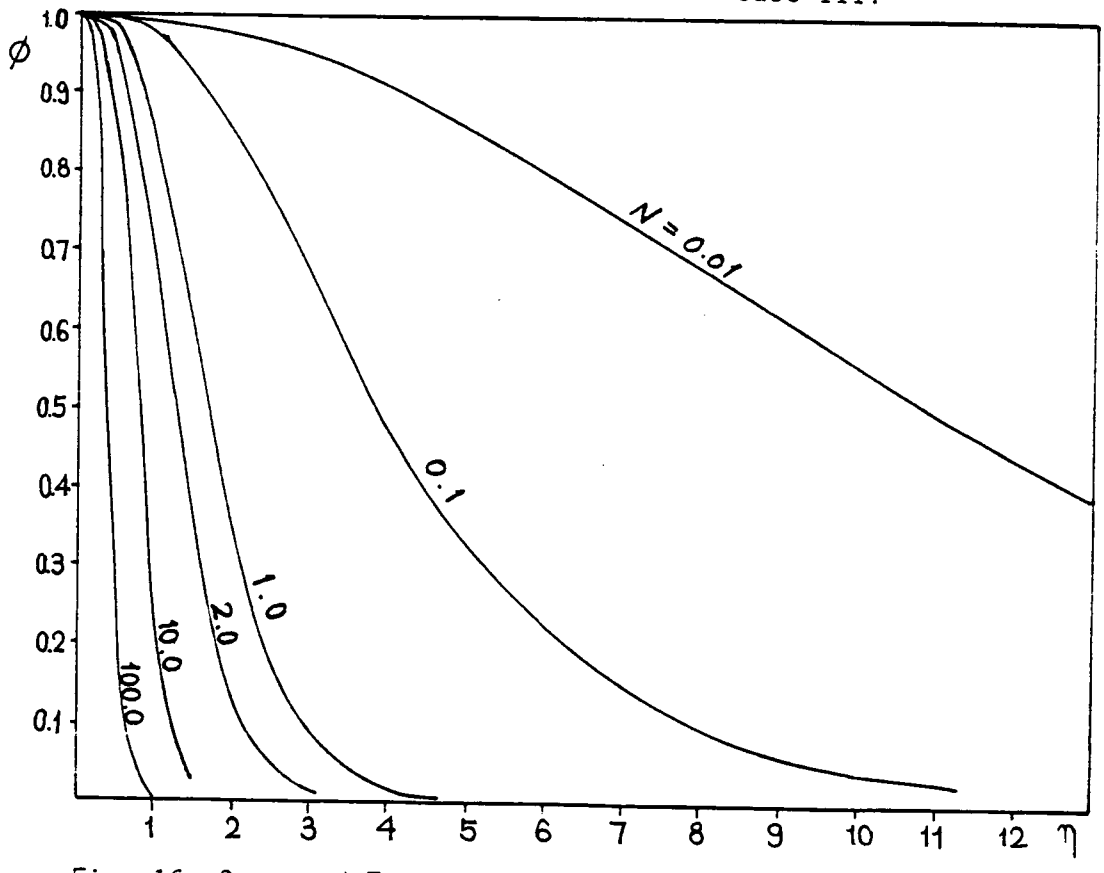


Fig. 16. Computed Temperature Distribution for Case III.

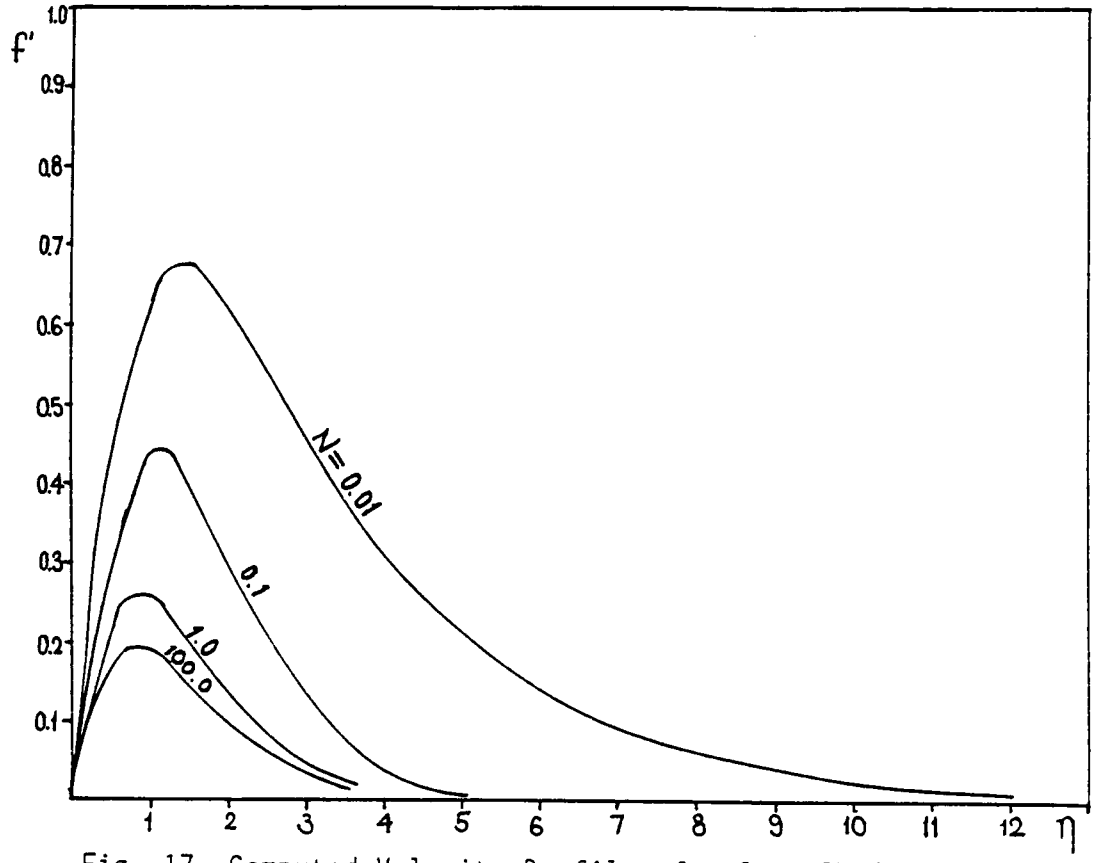


Fig. 17. Computed Velocity Profiles for Case IV (Pr=10.0).

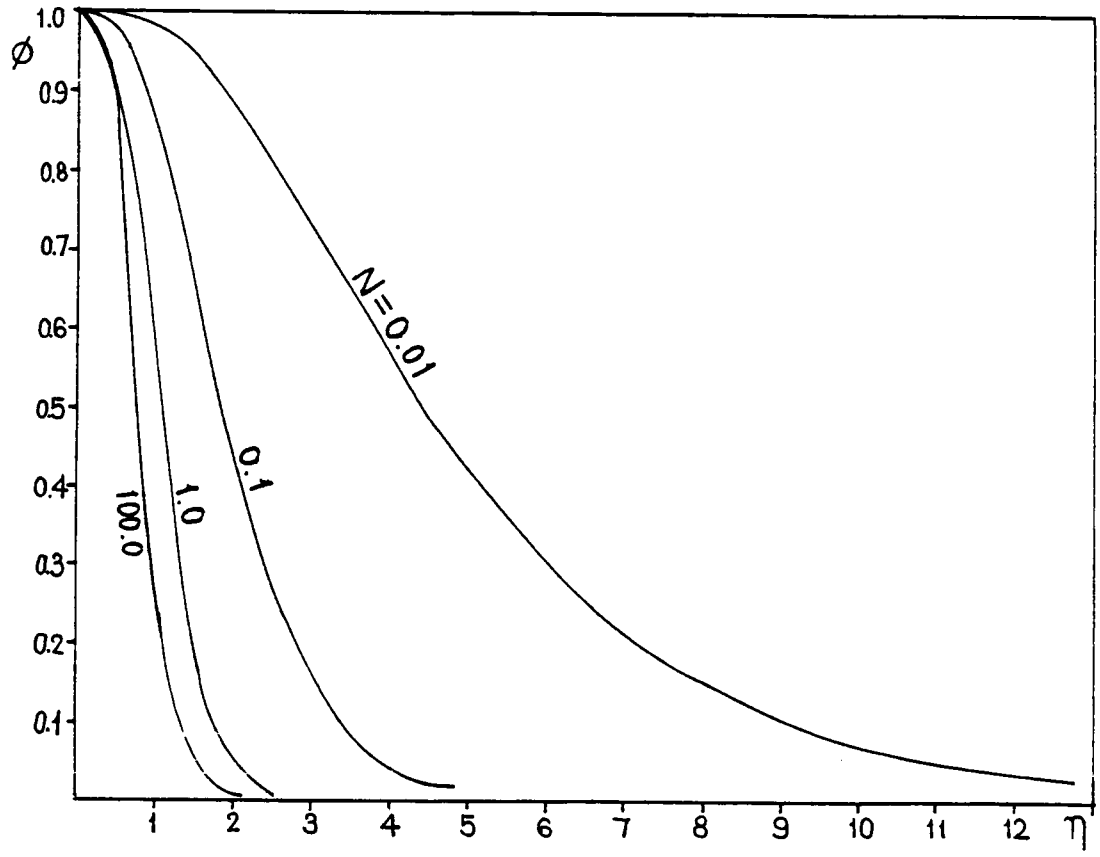


Fig. 18. Computed Temperature Distribution for Case IV (Pr=10.0).

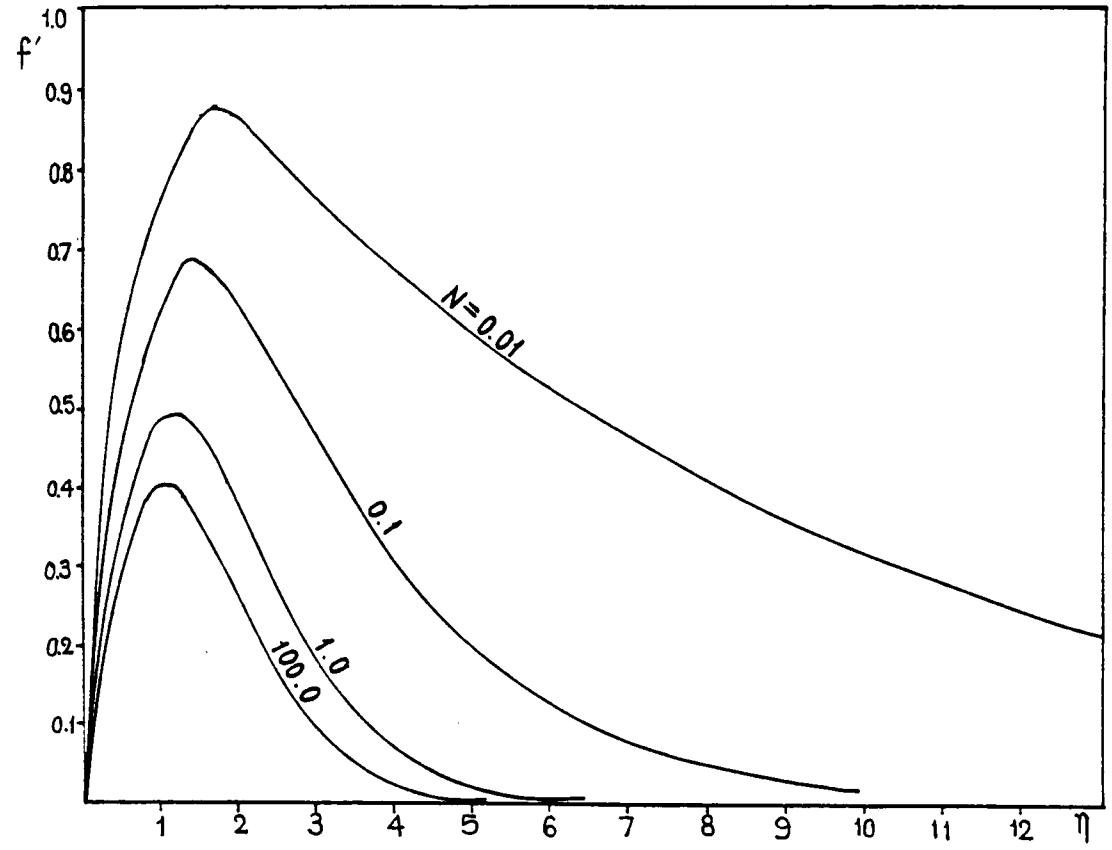


Fig. 19. Computed Velocity Profiles for Case IV (Pr=1.0).

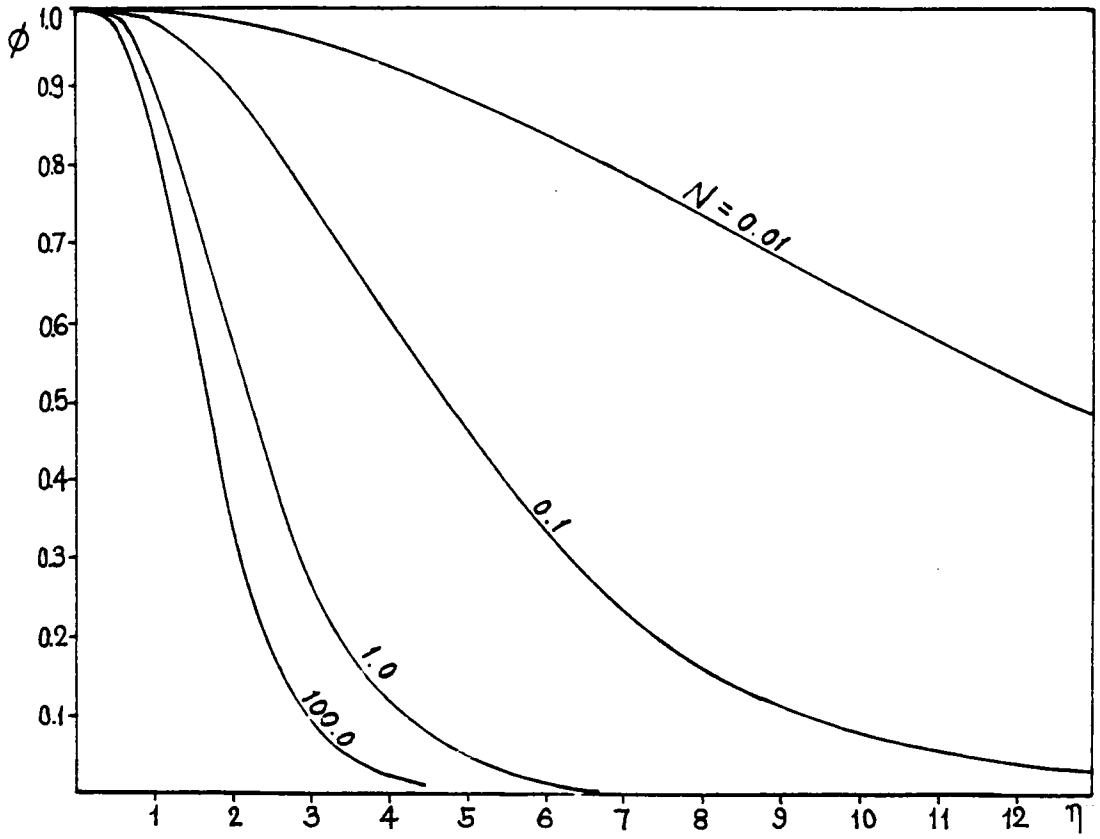


Fig. 20. Computed Temperature Distribution for Case IV (Pr=1.0)

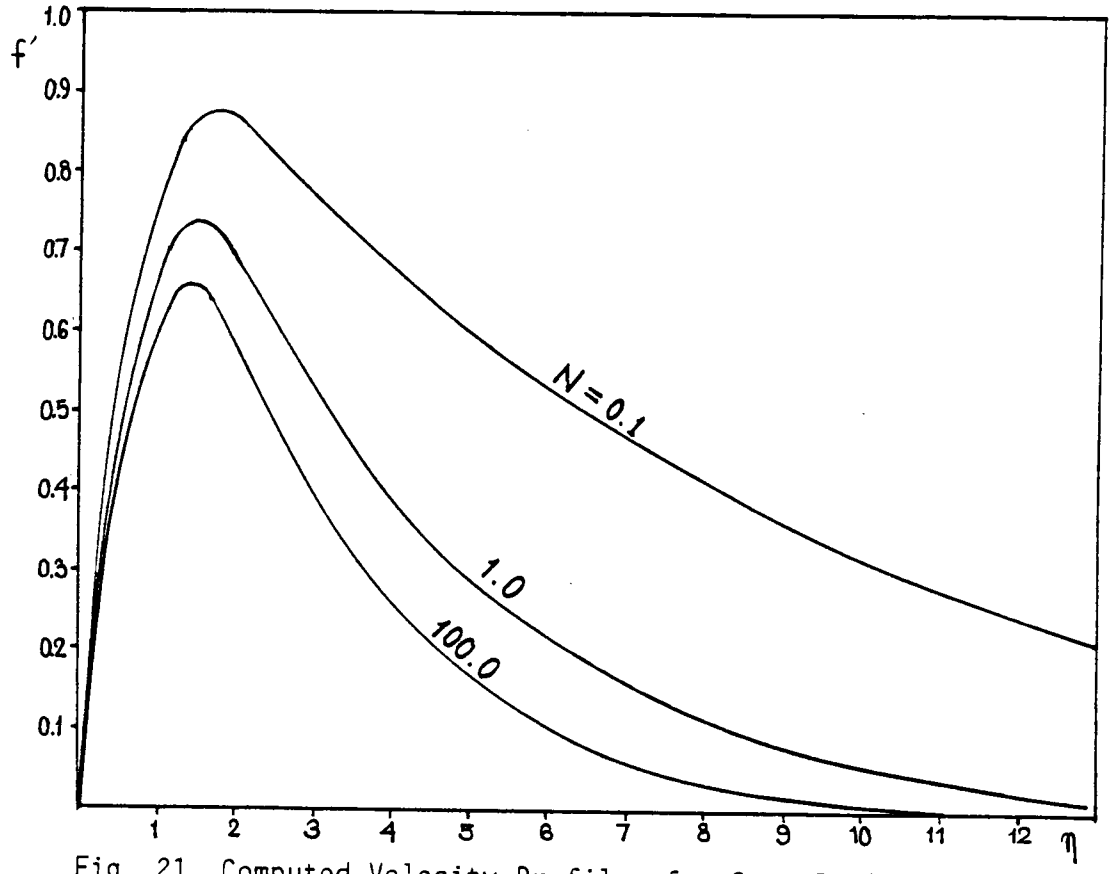


Fig. 21. Computed Velocity Profiles for Case IV (Pr=0.1).

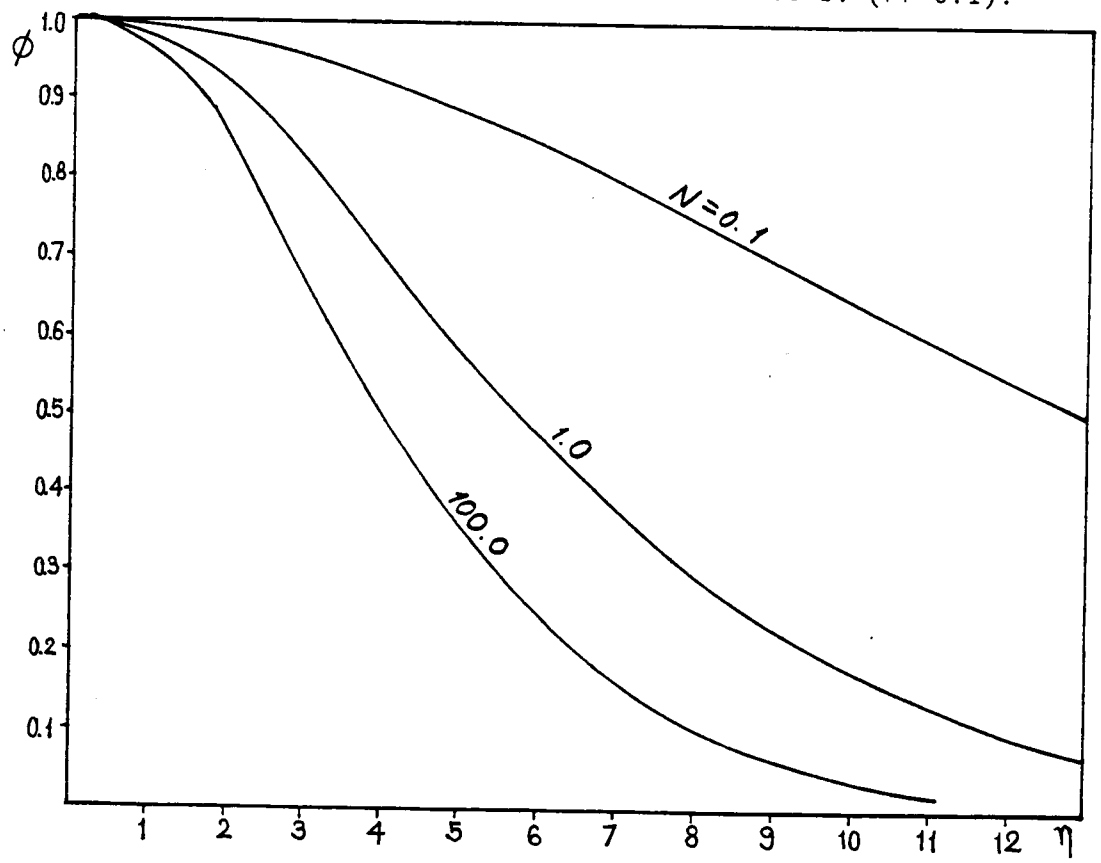


Fig. 22. Computed Temperature Distribution for Case IV (Pr=0.1).

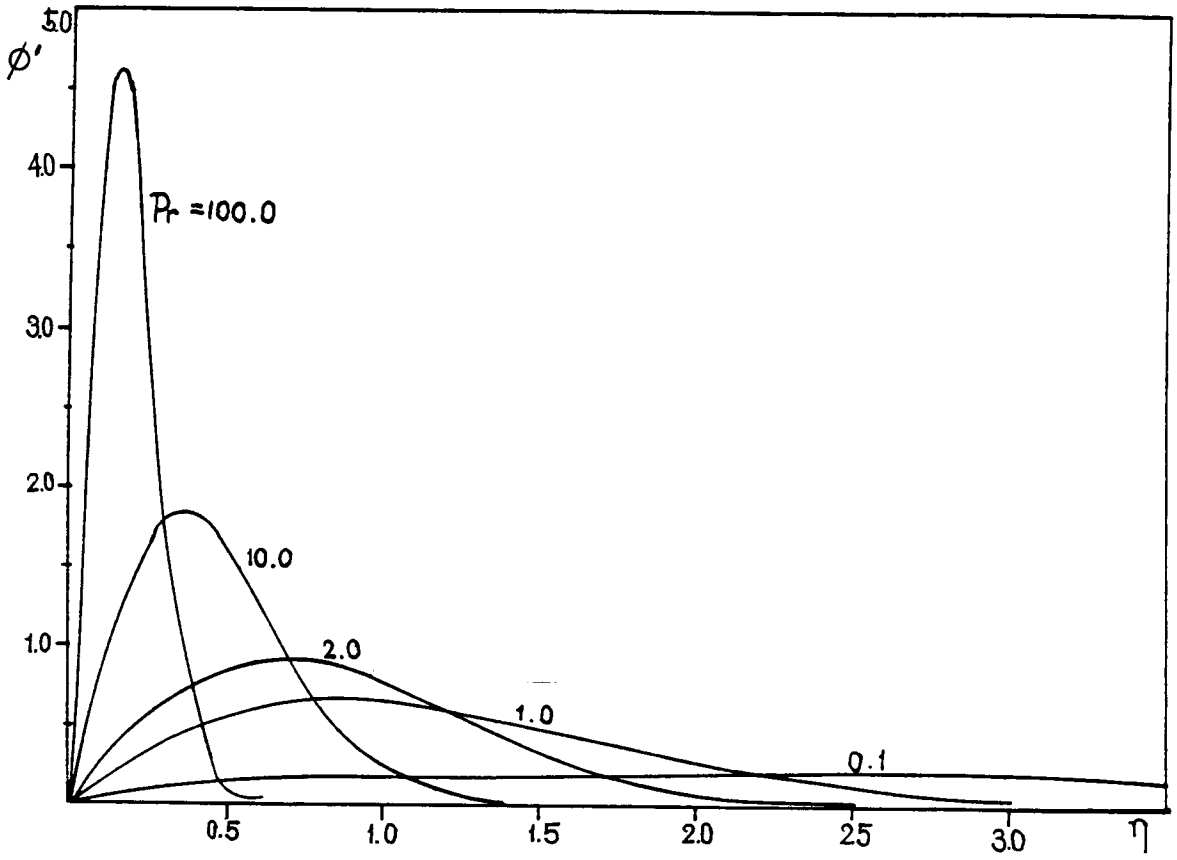


Fig. 23. Temperature Gradients across the Boundary Layer for Case I.

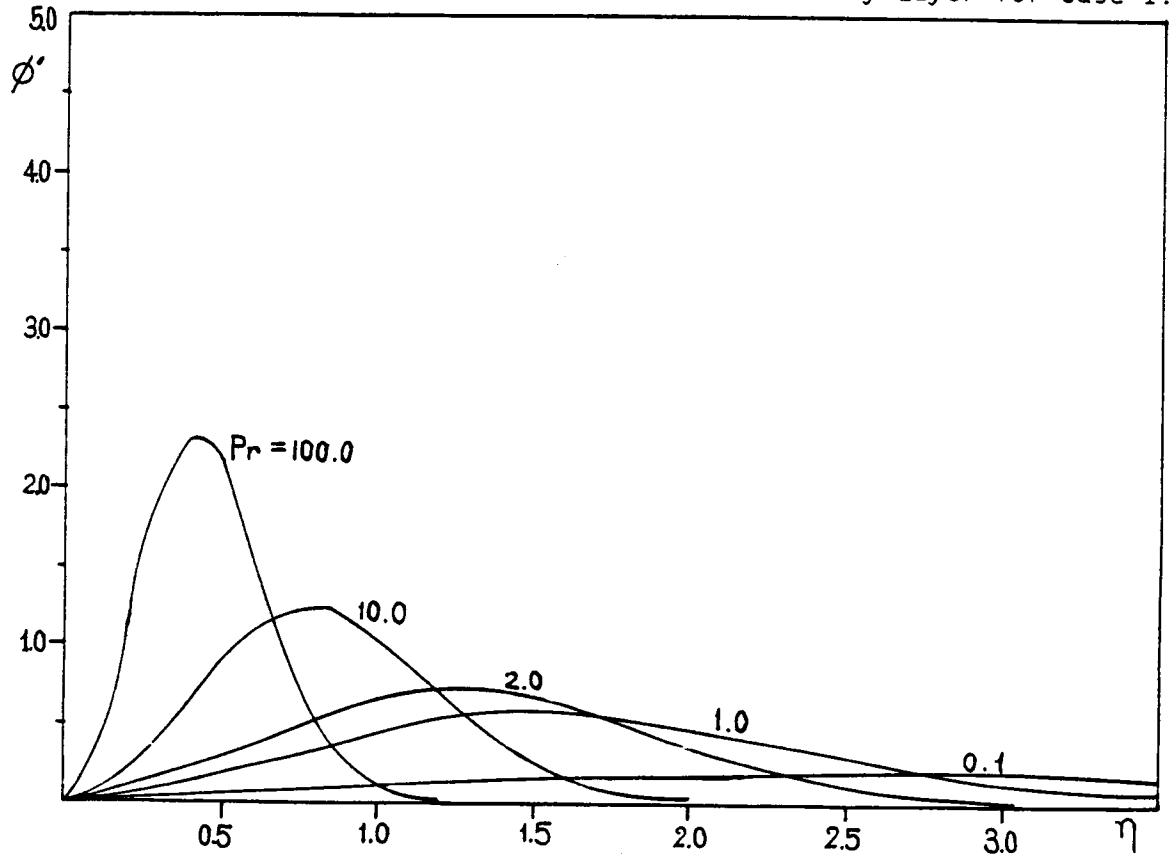


Fig. 24. Temperature Gradients across the Boundary Layer for Case III.

APPENDIX B

ADDITIONAL TABLES

Table 5. Comparison of Numerical Values of Computed Dimensionless Velocity f'(0) for Case I.

Pr		0.01	0.1	1.0	2.0	10.0	100.0
f'	Calculated in this paper	0.9817	0.8401	0.6255	0.5592	0.4094	0.2033
	Calculated by Gebhart et.al	0.9751	o.8408	0.6265	0.5590	0.4139	0.2505

Table 6. The Dimensionless Shear Stress on the Vertical Wall.

	Pr	N	f"(0)
CASE III	0.01		1.3004
	0.1		1.1361
	1.0		0.8863
	2.0		0.8037
	10.0		0.6061
	100.0		0.3691
CASE IV	0.1	0.1	1.3159
		1.0	1.2079
		100.0	1.1373
	1.0	0.01	1.3152
		0.1	1.1682
		1.0	0.9854
		100.0	0.8879
	10.0	0.01	1.1634
		0.1	0.9284
		1.0	0.7074
		100.0	0.6076

Table 7. Comparison of the Effect of an Adiabatic Vertical Wall on Temperature Gradients for the First and Third Cases.

Pr	100.0		1.0		0.01	
η CASE	I	III	I	III	I	III
0.0	1.0000	1.0000	1.0000	1.0000	1.0000	1.0000
0.1	0.7924	0.9901	0.9934	0.9997	0.999895	0.999996
0.2	0.3985	0.9292	0.9753	0.9980	0.999607	0.999970
0.3	0.1290	0.7940	0.9465	0.9935	0.9991	0.9999
0.4	0.0272	0.6017	0.9081	0.9853	0.9985	0.9998
0.5	0.0035	0.3984	0.8617	0.9725	0.9976	0.9996
0.6		0.2293	0.8087	0.9544	0.9966	0.9993
0.7		0.1147	0.7517	0.9308	0.9954	0.9987
0.8		0.0500	0.6918	0.9016	0.9940	0.9984
0.9		0.0190	0.6310	0.8671	0.9924	0.9977
1.0		0.0063	0.5706	0.8277	0.9908	0.9969
1.5			0.3101	0.5854	0.9797	0.9909
2.0			0.1484	0.3487	0.9650	0.9809
3.0			0.0279	0.0881	0.9260	0.9500
4.0			0.0042	0.0177	0.8772	0.9074
5.0				0.0086	0.8218	0.8562
7.0					0.7014	0.7397
10.0					0.5245	0.5609

APPENDIX C

FORTRAN PROGRAM

COMPUTER PROGRAM FOR CASE II

```
      IMPLICIT REAL*8(A-H,O-Z), INTEGER(I-N)
      DIMENSION YS(50),Y(50),Q(50),XI(30),FF(12,500),GG(12,500)
      COMMON/PARAMT/PN,RN,GW
      EMAX=0.05
      PR=0.1
      PNN=0.01
      DX=0.05
      WRITE(5,99) EMAX,PR,PNN,DX
      WRITE(22,99) EMAX,PR,PNN,DX
   99 FORMAT(/////
     &   ,10X,'*****************************************************'
     & ,/,10X,'*                                                   *'
     & ,/,10X,'* THE SOLUTION FOR THE STEADY LAMINAR NATURAL      *'
     & ,/,10X,'* CONVECTION PLUMES ABOVE A  HORIZONTAL            *'
     & ,/,10X,'* LINE HEAT SOURCE WITH RADIATION EFFECT.          *'
     & ,/,10X,'*                                                   *'
     & ,/,10X,'*****************************************************'
     & ,///
     & ,/,10X,'*****************************************************'
     & ,/,10X,'*                                                   *'
     & ,/,10X,'*          EMAX=',F9.5, '                           *'
     & ,/,10X,'*          PR  =',F9.5, '                           *'
     & ,/,10X,'*          PNN =',F9.5 ,'                           *'
     & ,/,10X,'*          DX  =',F9.5, '                           *'
     & ,/,10X,'*                                                   *'
     & ,/,10X,'*****************************************************'
     & ,////)
      PN=1.00D0
      DZMAX=0.1D+01
      DWMAX=0.1D+01
      N=15
      NDNF=60
      NDXW=2
      NF=2
      Z=1.08D0
      ISFW=0
      RN=4.D0/(3.D0*PNN)
    1 XS=0.D0
      YS(1)=0.D0
      YS(2)=Z
      YS(3)=0.0
      YS(4)=1.
      YS(5)=0.0
```

```
      YS(6)=0.D0
      YS(7)=1.D0
      YS(8)=0.D0
      YS(9)=0.D0
      YS(10)=0.D0
      YS(11)=0.D0
      YS(12)=0.D0
      YS(13)=0.D0
      YS(14)=0.D0
      YS(15)=0.00
      IF(ISFW-5) 34,34,200
  200 WRITE(5,55)
      WRITE(22,55)
   55 FORMAT(4X ,'Y',7X,'F',12X,'DF',11X,'DDF',11X,'G',11X,'DG',/
     &)
      WRITE(5,201) XS,YS(1),YS(2),YS(3),YS(4),YS(5)
      WRITE(22,201) XS,YS(1),YS(2),YS(3),YS(4),YS(5)
  201 FORMAT(F7.3,5D13.6)
   34 ISR=0
      INF=1
    3 CALL RNKTGL(N,ISR,XS,DX,NDXW,YS,XFC,Y,Q,PR)
      IF(ISFW-5) 45,45,300
  300 WRITE(5,201) XFC,Y(1),Y(2),Y(3),Y(4),Y(5)
      WRITE(22,201) XFC,Y(1),Y(2),Y(3),Y(4),Y(5)
   45 IF(INF-NDNF) 4,5,5
    4 INF=INF+1
      ISR=ISR+1
      GO TO 3
    5 A1=Y(7)**2+Y(9)**2+Y(8)**2+Y(10)**2
      C1=-(+Y(2)*Y(7)+Y(4)*Y(9)+Y(3)*Y(8)+Y(5)*Y(10))
      DZ=C1/A1
      E=Y(2)**2+Y(3)**2+Y(4)**2+Y(5)**2
      Z=Z+DZ
      IF(DABS(DZ/Z).GT.DZMAX) GO TO 1
      IF(E-EMAX) 13,14,14
   14 NDNF=NDNF+NF
      GO TO 1
   13 IF(ISFW-5) 401,401,402
  401 ISFW=ISFW+10
      Z=Z-DZ
      GO TO 1
  402 WRITE(5,203) E
      WRITE(22,203) E
  203 FORMAT(///,15X,'**** E=',D16.8,'*****',//)
      WRITE(5,66)
      WRITE(22,66)
   66 FORMAT(///,30X,'YEUNSIK CHOI',/,
     &           30X,'DEPT.OF ENGINEERING SCIENCE & MECHANICS',/,
     &           30X,'THE UNIVERSITY OF TENNESSEE, KNOXVILLE.',/
     &////)
      STOP
      END
```

```
      SUBROUTINE RNKTGL(N,ISR,XS,DX,NDXW,YS,XFC,Y,Q,PR)
      IMPLICIT REAL*8(A-H,O-Z),INTEGER(I-N)
      DIMENSION YS(50),F(50),Y(50),Q(50)
      COMMON/PARAMT/PN,RN,GW
      A1=0.5D+00
      A2=0.1D+01-DSQRT(0.5D+00)
      A3=0.1D+01+DSQRT(0.5D+00)
      A4=0.1D+01/0.6D+01
      IF (ISR) 1,1,3
    1 X=XS
      DO 2 I=1,N
      Y(I)=YS(I)
      Q(I)=0.
    2 CONTINUE
    3 IDX=1
    5 CALL FNLIST (X,Y,F,PR)
      DO 10 I=1,N
      DK1=DX*F(I)
      Y(I)=Y(I)+A1*(DK1-0.2D+01*Q(I))
      Q(I)=Q(I)+0.3D+01*A1*(DK1-0.2D+01*Q(I))-A1*DK1
   10 CONTINUE
      X=X+0.5D+00*DX
      CALL FNLIST (X,Y,F,PR)
      DO 20 I=1,N
      DK2=DX*F(I)
      Y(I)=Y(I)+A2*(DK2-Q(I))
      Q(I)=Q(I)+0.3D+01*A2*(DK2-Q(I))-A2*DK2
   20 CONTINUE
      CALL FNLIST (X,Y,F,PR)
      DO 30 I=1,N
      DK3=DX*F(I)
      Y(I)=Y(I)+A3*(DK3-Q(I))
      Q(I)=Q(I)+0.3D+01*A3*(DK3-Q(I))-A3*DK3
   30 CONTINUE
      X=X+0.5D+00*DX
      CALL FNLIST (X,Y,F,PR)
      DO 40 I=1,N
      DK4=DX*F(I)
      Y(I)=Y(I)+A4*(DK4-0.2D+01*Q(I))
      Q(I)=Q(I)+0.3D+01*A4*(DK4-0.2D+01*Q(I))-A4*DK4
   40 CONTINUE
      IF (IDX-NDXW) 41,42,42
   41 IDX=IDX+1
      GO TO 5
   42 XFC=X
      RETURN
      END
```

```
      SUBROUTINE FNLIST(X,Y,F,PR)
      IMPLICIT REAL*8(A-H,O-Z),INTEGER(I-N)
      DIMENSION Y(50),F(50)
      COMMON/PARAMT/PN,RN,GW
      RNN=1.D0+RN
      RNY1=1.D0+RN*Y(4)**3
      RNY2=RNY1*RNY1
      F(1)=Y(2)
      F(2)=Y(3)
      F(3)=-(2.4)*Y(1)*Y(3)+(0.8)*(Y(2)**2)-Y(4)
      F(4)=Y(5)
      F(5)=-(2.4)*PR*(Y(2)*Y(4)+Y(1)*Y(5))/RNN
      F(6)=Y(7)
      F(7)=Y(8)
      F(8)=-(2.4)*(Y(6)*Y(3)+Y(1)*Y(8))+(1.6)*Y(2)*Y(6)-Y(9)
      F(9)=Y(10)
      F(10)=-(2.4)*PR*(Y(7)*Y(4)+Y(2)*Y(9)+Y(6)*Y(5)+Y(1)*Y(10))/RNN
      F(11)=Y(12)
      F(12)=Y(13)
      F(13)=-(2.4)*(Y(11)*Y(3)+Y(1)*Y(13))+(1.6)*Y(2)*Y(11)-Y(14)
      F(14)=Y(15)
      F(15)=-(2.4)*PR*(Y(12)*Y(4)+Y(2)*Y(14)+Y(11)*Y(5)+Y(1)*Y(15))
     &/RNN
9999  CONTINUE
      RETURN
      END
```

COMPUTER PROGRAM FOR CASE III

```
      IMPLICIT REAL*8(A-H,O-Z), INTEGER(I-N)
      DIMENSION YS(50),Y(50),Q(50),XI(30),FF(12,500),GG(12,500)
      COMMON/PARAMT/PN,RN,GW
      EMAX=0.001
      PR=0.1
      DX=0.05
      WRITE(5,99) EMAX,PR,DX
      WRITE(23,99) EMAX,PR,DX
   99 FORMAT(/////
     &    ,10X,'*****************************************************'
     & ,/,10X,'*                                                   *'
     & ,/,10X,'* THE SOLUTION FOR THE STEADY LAMINAR NATURAL        *'
     & ,/,10X,'* CONVECTION PLUMES ABOVE A HORIZONTAL LINE HEAT     *'
     & ,/,10X,'* A HORIZONTAL LINE HEAT SOURCE WITH AN INSULATED    *'
     & ,/,10X,'* VERTICAL WALL AND WITHOUT RADIATION EFFECT.        *'
     & ,/,10X,'*                                                   *'
     & ,/,10X,'*****************************************************'
     & ,///
     & ,/,10X,'*****************************************************'
     & ,/,10X,'*                                                   *'
     & ,/,10X,'*          EMAX=',F9.5,' '                          *'
     & ,/,10X,'*          PR  =',F9.5,' '                          *'
     & ,/,10X,'*          DX  =',F9.5,' '                          *'
     & ,/,10X,'*                                                   *'
     & ,/,10X,'*****************************************************'
     & ,////)
      PNN=1.0
      DZMAX=0.1D+01
      DWMAX=0.1D+01
      N=15
      NDNF=60
      NDXW=2
      NF=2
      Z=1.08D0
      ISFW=0
      RN=4.D0/(3.D0*PNN)
      WRITE(5,55)
      WRITE(23,55)
   55 FORMAT(4X,'Y',7X,'F',12X,'DF',11X,'DDF',11X,'G',11X,'DG',/)
    1 XS=0.D0
      YS(1)=0.D0
      YS(2)=0.D0
      YS(3)=Z
      YS(4)=1.
      YS(5)=0.0
```

```
      YS(6)=0.D0
      YS(7)=0.D0
      YS(8)=1.D0
      YS(9)=0.D0
      YS(10)=0.D0
      YS(11)=0.D0
      YS(12)=0.D0
      YS(13)=0.D0
      YS(14)=0.D0
      YS(15)=0.00
      IF(ISFW-5) 34,34,200
  200 WRITE(5,201) XS,YS(1),YS(2),YS(3),YS(4),YS(5)
      WRITE(23,201) XS,YS(1),YS(2),YS(3),YS(4),YS(5)
  201 FORMAT(F7.3,5D13.6)
   34 ISR=0
      INF=1
    3 CALL RNKTGL(N,ISR,XS,DX,NDXW,YS,XFC,Y,Q,PR)
      IF(ISFW-5) 45,45,300
  300 WRITE(5,201) XFC,Y(1),Y(2),Y(3),Y(4),Y(5)
      WRITE(23,201) XFC,Y(1),Y(2),Y(3),Y(4),Y(5)
   45 IF(INF-NDNF) 4,5,5
    4 INF=INF+1
      ISR=ISR+1
      GO TO 3
    5 A1=Y(7)**2+Y(9)**2+Y(8)**2+Y(10)**2
      C1=-(+Y(2)*Y(7)+Y(4)*Y(9)+Y(3)*Y(8)+Y(5)*Y(10))
      DZ=C1/A1
      E=Y(2)**2+Y(3)**2+Y(4)**2+Y(5)**2
      Z=Z+DZ
      IF(DABS(DZ/Z).GT.DZMAX ) GO TO 1
      IF(E-EMAX) 13,14,14
   14 NDNF=NDNF+NF
      GO TO 1
   13 IF(ISFW-5) 401,401,402
  401 ISFW=ISFW+10
      Z=Z-DZ
      GO TO 1
  402 WRITE(5,203) E
      WRITE(23,203) E
  203 FORMAT(///,15X,'***** E=',D16.8,'*****',//
     &       ///,30X,'YEUNSIK CHOI',/,
     &           30X,'DEPT. OF ENGINEERING SCIENCE & MECHANICS',/,
     &           30X,'THE UNIV. OF TENNESSEE, KNOXVILLE.',/////)
      STOP
      END
```

```
      SUBROUTINE RNKTGL(N,ISR,XS,DX,NDXW,YS,XFC,Y,Q,PR)
      IMPLICIT REAL*8(A-H,O-Z),INTEGER(I-N)
      DIMENSION YS(50),F(50),Y(50),Q(50)
      COMMON/PARAMT/PN,RN,GW
      A1=0.5D+00
      A2=0.1D+01-DSQRT(0.5D+00)
      A3=0.1D+01+DSQRT(0.5D+00)
      A4=0.1D+01/0.6D+01
      IF (ISR) 1,1,3
    1 X=XS
      DO 2 I=1,N
      Y(I)=YS(I)
      Q(I)=0.
    2 CONTINUE
    3 IDX=1
    5 CALL FNLIST (X,Y,F,PR)
      DO 10 I=1,N
      DK1=DX*F(I)
      Y(I)=Y(I)+A1*(DK1-0.2D+01*Q(I))
      Q(I)=Q(I)+0.3D+01*A1*(DK1-0.2D+01*Q(I))-A1*DK1
   10 CONTINUE
      X=X+0.5D+00*DX
      CALL FNLIST (X,Y,F,PR)
      DO 20 I=1,N
      DK2=DX*F(I)
      Y(I)=Y(I)+A2*(DK2-Q(I))
      Q(I)=Q(I)+0.3D+01*A2*(DK2-Q(I))-A2*DK2
   20 CONTINUE
      CALL FNLIST (X,Y,F,PR)
      DO 30 I=1,N
      DK3=DX*F(I)
      Y(I)=Y(I)+A3*(DK3-Q(I))
      Q(I)=Q(I)+0.3D+01*A3*(DK3-Q(I))-A3*DK3
   30 CONTINUE
      X=X+0.5D+00*DX
      CALL FNLIST (X,Y,F,PR)
      DO 40 I=1,N
      DK4=DX*F(I)
      Y(I)=Y(I)+A4*(DK4-0.2D+01*Q(I))
      Q(I)=Q(I)+0.3D+01*A4*(DK4-0.2D+01*Q(I))-A4*DK4
   40 CONTINUE
      IF (IDX-NDXW) 41,42,42
   41 IDX=IDX+1
      GO TO 5
   42 XFC=X
      RETURN
      END
```

```
      SUBROUTINE FNLIST(X,Y,F,PR)
      IMPLICIT REAL*8(A-H,O-Z),INTEGER(I-N)
      DIMENSION Y(50),F(50)
      COMMON/PARAMT/PN,RN,GW
      RNN=1.D0+RN
      RNY1=1.D0+RN*Y(4)**3
      RNY2=RNY1*RNY1
      F(1)=Y(2)
      F(2)=Y(3)
      F(3)=-(2.4)*Y(1)*Y(3)+(0.8)*(Y(2)**2)-Y(4)
      F(4)=Y(5)
      F(5)=-(2.4)*PR*(Y(2)*Y(4)+Y(1)*Y(5))
      F(6)=Y(7)
      F(7)=Y(8)
      F(8)=-(2.4)*(Y(6)*Y(3)+Y(1)*Y(8))+(1.6)*Y(2)*Y(6)-Y(9)
      F(9)=Y(10)
      F(10)=-(2.4)*PR*(Y(7)*Y(4)+Y(2)*Y(9)+Y(6)*Y(5)+Y(1)*Y(10))
      F(11)=Y(12)
      F(12)=Y(13)
      F(13)=-(2.4)*(Y(11)*Y(3)+Y(1)*Y(13))+(1.6)*Y(2)*Y(11)-Y(14)
      F(14)=Y(15)
      F(15)=-(2.4)*PR*(Y(12)*Y(4)+Y(2)*Y(14)+Y(11)*Y(5)+Y(1)*Y(15))
 9999 CONTINUE
      RETURN
      END
```

VITA

Yeunsik Choi was born in Daegu, Korea on October 18, 1960. He attended elementary schools in that city and in Seoul. He graduated from Soong-Sil Middle school in 1976. In the following March, he attended the High School attached to the College of Education of Choong-Ang University. In 1979 he entered Ajou University in Suweon, Korea, and received a Bachelor of Science degree in Mechanical engineering in Feburary 1983. During his undergraduate study, he was awarded the scholarship for excellent students from the university.

In the fall of 1983, he began to study at the University of Tennessee, Knoxville, as a graduate teaching asistant. He received the Master of Science degree with a major in Engineering Science and Mechanics in June, 1985. The author is a member of the American Society of Mechanical Engineers, and the American Institute of Aeronautics and Astrounautics.